Digital Predistortion for Broadband Radio-over-Fiber Transmission Systems

Zichen Xuan

A Thesis

in

The Department

of

Electrical and Computer Engineering

Presented in Partial Fulfillment of the Requirements

For the Degree of Master of Applied Science at

Concordia University

Montréal, Québec, Canada

Sept. 2015

CONCORDIA UNIVERSITY
SCHOOL OF GRADUATE STUDIES

This is to certify that the thesis prepared

By: Zichen Xuan

Entitled: "Digital Predistortion for Broadband Radio-over-Fiber Transmission Systems"

and submitted in partial fulfillment of the requirements for the degree of

Master of Applied Science

Complies with the regulations of this University and meets the accepted standards with respect to originality and quality.

Signed by the final examining committee:

_____ Chair
Dr. R. Raut

_____ Examiner, External
Dr. C. Assi (CIISE) To the Program

_____ Examiner
Dr. W-P. Zhu

_____ Supervisor
Dr. X. Zhang

Approved by: _____
Dr. W. E. Lynch, Chair
Department of Electrical and Computer Engineering

_____20_____ _____
Dr. Amir Asif, Dean
Faculty of Engineering and Computer Science

Abstract

Digital Predistortion for Broadband Radio-over-Fiber Transmission Systems

Zichen Xuan

Concordia University 2015

With the increase of the demand of high capacity wireless access, design of cost effective broadband wireless signal distribution system is required, particularly for future massive multi-input and multi-output (MIMO) wireless. Recently, Radio-over-Fiber (RoF) transmission systems have been revisited for broadband wireless signal distribution between central processing unit (CPU) and remote radio unit (RRU) (i.e., antenna towers). RoF, which is based on optical subcarrier modulation and thus an analog transmission system, fully utilize the advantages of broadband and low-loss fiber transmission, and also radio signal transmission.

Unfortunately, RoF transmission systems are very susceptible to nonlinear distortions, which can be generated by all inline functional components of the RoF systems. However, two typical functions, i.e., optical subcarrier modulation and RF power amplification, are the two key sources of the nonlinear distortions. Various linearization techniques have been investigated for power RF amplifiers. It has been found that digital predistortion (DPD) linearization is one of the best approaches for RF bandwidth of up to 20 MHz.

In this thesis, DPD linearization is explored for broadband RoF transmission systems. Instead of DPD implemented in baseband previously, a DPD linearization technique implemented in RF domain is investigated and demonstrated experimentally for broadband RoF transmission systems. Memory polynomial (MP) model is used for theoretical modeling of nonlinear RoF transmission systems, in which both nonlinear distortion and

memory effect can be included. In order to implement the predistorter of the DPD using the MP model, least square (LS) method is used to extract the coefficients of the predistorter. Using the obtained coefficients, the trained predistorter is implemented and then verified in two experiments of directly modulated RoF transmission systems. In the first experiment, the DPD is verified in WiFi over fiber transmission systems, and more than 8 dB and 5.6 dB improvements of error vector magnitude (EVM) are achieved in back to back (BTB) and after 10 km single mode fiber (SMF) transmission. In the second experiment, both WiFi and ultra wide band (UWB) wireless signals are transmitted in the RoF system, which occupies over 2.4 GHz transmission bandwidth. It is shown that the implemented DPD leads to EVM improvements of 4.5 dB (BTB) and 3.1 dB (10 km SMF) for the WiFi signal, and 4.6 dB (BTB) and 4 dB (10 km SMF) for the UWB signal.

Acknowledgement

I would like to express my sincere gratitude to Professor Xiupu Zhang for his guidance, inspiration and being thoughtful all the time. It's been an honor to work and finish this thesis under his supervision.

My thanks also goes to Ran Zhu, Hakim Mellah, who gave me a lot of ideas and suggestions while I was doing the experiments. Also, I want to thank my friend Hang Chen for all his help in the past three years.

Last but not least, I would like to thank my parents: Liping Xuan and Shujuan Sun for their endless love and spiritual support in all my life. Without you, I would never have a chance to finish this work. I thank my lovely girlfriend Jiawei Wu for all her encouragements and tasty dishes through thick and thin.

Table of contents

List of figures

List of Acronyms

ACP	Adjacent Channel Power
ADC	Analog to Digital Converter
AWG	Arbitrary Waveform Generator
CD	Chromatic Dispersion
CPU	Central Processing Unit
CW	Continuous Wave
DC	Direct Current
DPC	Digital Post Compensation
DR	Dynamic Range
DS-UWB	Direct Sequence Ultra Wideband
DSB	Double Sideband
DSL	Digital Subcarrier Line
DSP	Digital Signal Processing
EAM	Electro-Absorption Modulator
EML	Electro-absorption Modulation Laser
E/O	Electrical to Optical
EVM	Error Vector Magnitude
FCC	Federal Communication Commission
HD	Harmonic Distortion
HD2	Second order Harmonic Distortion
HD3	Third order Harmonic Distortion

IMD	Intermodulation Distortion
IMD3	Third order Intermodulation Distortion
IMD5	Fifth order Intermodulation Distortion
LD	Laser Diode
LS	Least Square
MB-OFDM	Multi-band Orthogonal Frequency Division Multiplexing
MD	Modal Dispersion
MP	Memory Polynomial
MIMO	Multiple Input Multiple Output
MZM	Mach-Zehnder Modulator
NMSE	Normalized Mean Square Error
NF	Noise Figure
OFDM	Orthogonal Frequency Division Multiplexing
ORx	Optical Receiver
OTx	Optical Transmitter
PA	Power Amplifier
PD	Photodiode
PSD	Power Spectral Density
PSK	Phase Shift Keying
QAM	Quadrature Amplitude Modulation
RF	Radio Frequency
RRU	Remote Radio Unit
RoF	Radio over Fiber

SCM	Subcarrier Multiplexing
SFDR	Spurious-free Dynamic Range
SMF	Single Mode Fiber
SNR	Signal to Noise Ratio
SOA	Semiconductor Optical Amplifier
SSB	Single Sideband
UWB	Ultra Wide Band
VSG	Vector Signal Generator
WLAN	Wireless Local Area Network
WiMAX	Worldwide Interoperability for Microwave Access

List of Symbols

a_k	Nonlinear system coefficients
E	Square error
E_b	Bandgap energy
g	Gain
h	Plank Constant
h_k	Volterra kernel
K	Predistorter coefficients matrix
m	Memory variable
p	Nonlinear order
q	Memory depth
t	Time
T	Matrix transpose
U	Predistorter training block input matrix
v	Frequency
ω	Angular frequency
$x(n)$	Output of RoF transmission system
$x(n)/g$	Input of predistorter training block
$z(n)$	Input of RoF transmission system
$z(n)'$	Predistorter training block output

Chapter 1 Introduction

With the rapid development of advanced technologies, our modern life depends heavily on laptops, smart phones and tablets, more than ever before. These devices share one common feature: the demand of a high capacity wireless network. As shown in Figure 1-1, the back-haul and the front-haul transmission systems make-up the wireless access network. Basically, the back-haul system relies on high capacity digital fiber transmission. To distribute wireless signals to antenna towers in front-haul transmission systems, traditional technologies such as narrow band analog radio frequency (RF) transmission over coaxial cables and digital fiber transmissions are applied. However, microwave coaxial cables are too costly, and high frequency RF signals suffer from high attenuation in the cables. Moreover, digital fiber transmission technology has been investigated for years, but it still suffers from a serious drawback which is the complexity of the remote radio unit (RRU) site, since digital from and to analog signal processing is involved. Under these circumstances, Radio-over-Fiber (RoF) transmission systems provide a good solution for these disadvantages [1].

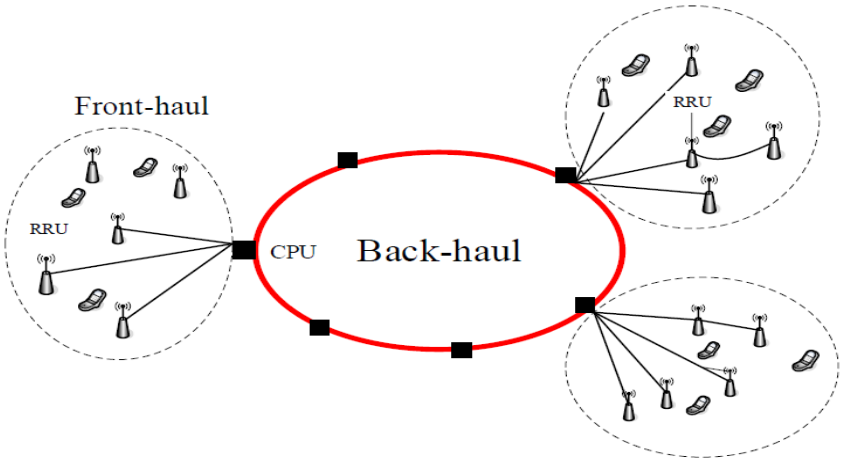

Figure 1-1 Infrastructure of wireless access network including back-haul and front-haul transmission systems [1].

1.1 Radio over Fiber (RoF)

Over two decades ago, A. J. Cooper firstly proposed and experimentally demonstrated RoF technology [2]. RoF systems transmit modulated light signals through optical fiber. With the growing demands of broadband wireless services and lower costs of optical components in recent years, RoF transmission systems have developed tremendous market advantages and attracted a large attention of research interests.

1.1.1 Basic configuration of RoF transmission system

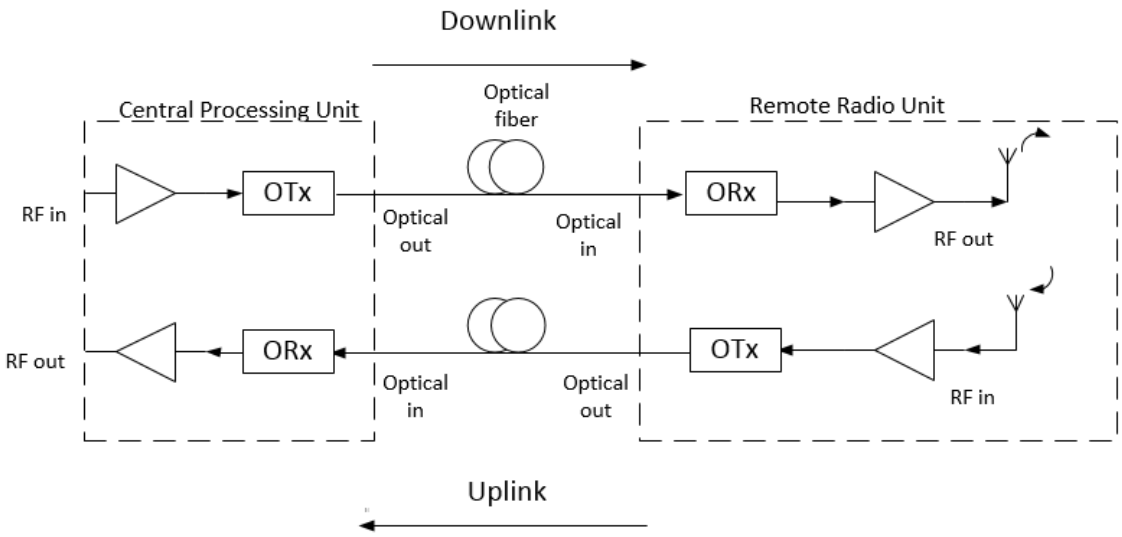

Figure 1-2 Configuration of RoF system.

The basic configuration of RoF transmission system is shown in Figure 1-2, consisting of the central processing unit (CPU) and the remote radio unit (RRU), which are both connected to each other by an optical fiber. The transmission direction from the CPU to the RRU is commonly phrased as *downlink*. An optical modulator in optical transmitter (OTx) is required to modulate the amplified RF signal to light signal. Laser Diode (LD) can be used as the direct optical modulator. To achieve larger modulation bandwidth, electro-absorption modulators (EAMs) and Mach–Zehnder modulators (MZMs) are also

widely used as the external optical modulators. Single mode fibers (SMFs) and multimode fibers can be used as the optical transmission media of RoF systems. After the transmission through optical fiber, an optical receiver (ORx) that transferring the carrier from optical to electrical domain is applied at RRU. The Photodiodes (PDs), which convert light to electrical signal, are widely used in ORx. Afterwards, the demodulated signal is amplified to feed an antenna, and information is finally distributed to users. Conversely, *uplink* is the opposite transmission direction to downlink. In this direction, the OTx converts RF signal received by antenna of RRU to light signal, then CPU can process RF signal demodulated by ORx [3-4].

1.1.2 Advantages of RoF transmission systems

RoF transmission systems support one CPU to multiple RRUs communication. In traditional transmission systems, all the frequency up/down conversion, frequency multiplexing and signal modulations are processed in the RRU. On the other hand, the RoF system has the advantage of centralizing most of signal processing procedures in the CPU, and the RRU has only the OTx, ORx, amplifier and antenna. As a result, this simplified device management of RRU reduces system complexity, power consumption and maintenance costs.

In addition, low attenuation and broad transmission bandwidth are the major advantages of RoF transmission systems. Using optical fiber instead of coaxial cable, the attenuation in signal transmission is much reduced. For instance, the SMFs have the optical attenuations of 0.5 dB/km at 1310 nm wavelength and 0.2 dB/km at 1550 nm wavelength, which are much lower than the RG-58 coaxial cable, which has the attenuation of 1056

dB/km. 850 nm, 1310 nm, and 1550 nm wavelengths are the three main transmission windows that offer low attenuation in optical fiber communications, and all of these three combined windows will result in a 50 THz transmission bandwidth. Furthermore, with the matured technologies such as wavelength division multiplexing (WDM) and sub-carrier multiplexing (SCM) being applied to optical communications, it is easy to realize the sufficient usage of the broad bandwidth of RoF transmission systems [5-8]. Apart from the advantages above, immunity to radio frequency interference and easy installation also render that RoF transmission systems will play a critical role in transmitting and distributing wireless signals in the future

1.1.3 Limitations of RoF transmission systems

In RoF systems, both analog modulations and detection of light are involved, therefore, the RoF transmission system is fundamentally an analog inclusive system, which means it can suffer from some of the analog communication systems' typical issues such as signal noises and nonlinear distortions. Major nonlinear distortion sources in RoF transmission systems include optical modulators and RF power amplifiers. These impairments result in the limitations of noise figure (NF) and dynamic range (DR). NF indicates the degradation of signal to noise ratio (SNR) of a system or a component, and it represents the quantity of noise which will be generated by the system or device. DR introduces the operational range of a system or a component, which is limited by the range from its noise floor to its compression point. DR is very important to mobile communications from RRUs to CPUs since the signal power received at RRU depends on the distance. For instance, within the same communication cell, compared to the RRU close to the CPU, the signal power received at a distant RRU is much smaller.

1.1.4 Optical subcarrier modulation

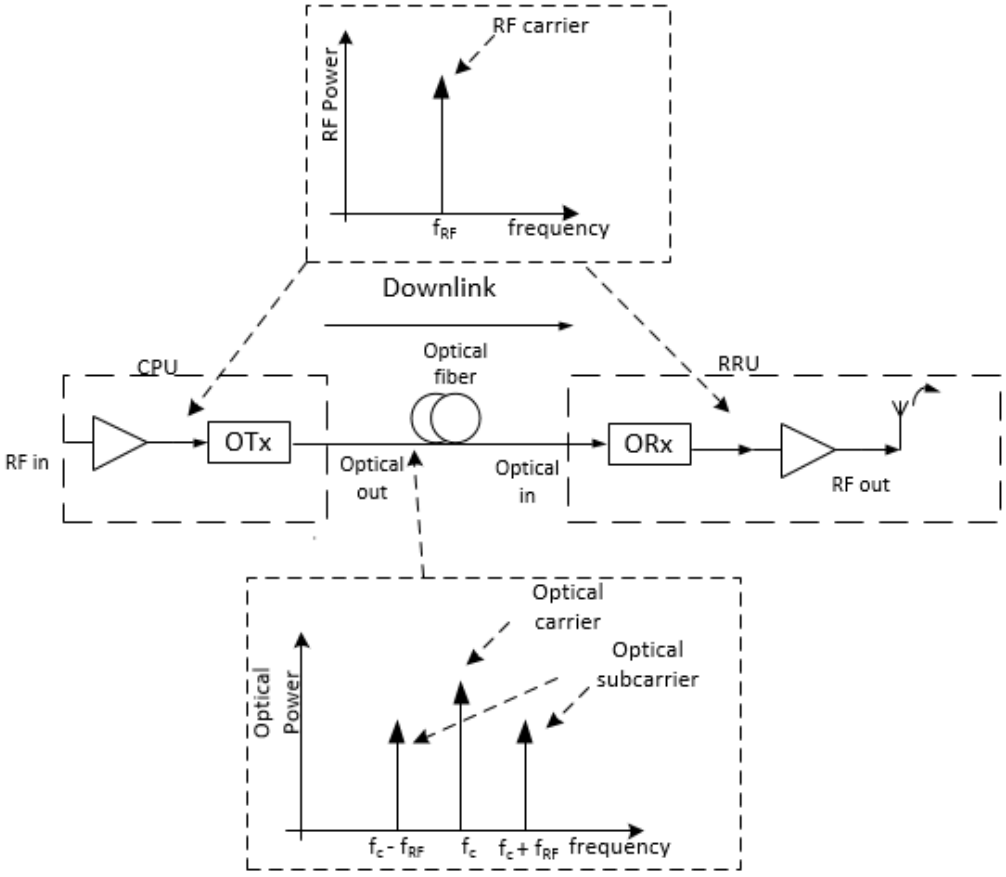

Figure 1-3 Principle of optical subcarrier modulation.

As discussed, RoF transmission systems have the advantages of transmitting and distributing RF signals. Taking RoF system downlink for example, as shown in Figure 1-3, an RF signal in the CPU is sent to modulate the optical signal in order to transmit information to the RRU. Then, optical subcarriers carry the RF signal in which the process is the optical subcarrier modulation. At the RRU, the received optical signal is converted back to the RF domain and amplified, after which information is finally distributed to the users by an antenna. As shown in Figure 1-4, optical subcarrier modulation can be realized by (a) direct modulation and (b) external modulation. Direct modulation uses only a laser, while external modulation uses a continuous wave (CW) laser and an external modulator

such as a MZM or an EAM. In comparison, direct modulation is simpler and cheaper than external modulation. However, direct modulation introduces a higher chirp which results in more chromatic dispersion (CD) effect. CD happens when two or more light signals with different frequencies are being transmitted in optical fiber, the arrival times of the transmitted signals are different.

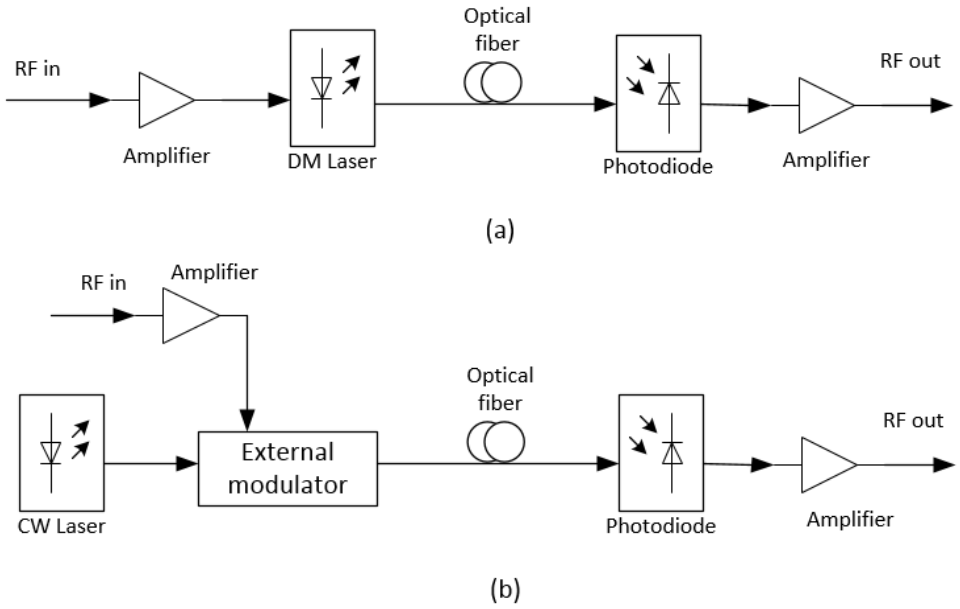

Figure 1-4 Optical subcarrier modulation (a) direct modulation and (b) external modulation.

Besides, as shown in Figure 1-3, the transmission of optical subcarriers occupies larger bandwidth than the transmission of RF carriers. This also makes the system more susceptible to CD since the broad transmission bandwidth is capable of transmitting more carriers. Thus, in order to reduce CD, other than using double sideband (DSB) modulation as shown in Figure 1-5 (a), single sideband (SSB) modulation, as shown in Figure1-5 (b) is investigated [9-10]. SSB modulation can be realized by biasing a dual-electrode MZM at quadrature and carefully controlling its phase difference. SSB modulation generates one

optical sub-band which is half of the modulation bandwidth of DSB modulation. The reduced modulation bandwidth of SSB modulation leads to the reduction of CD.

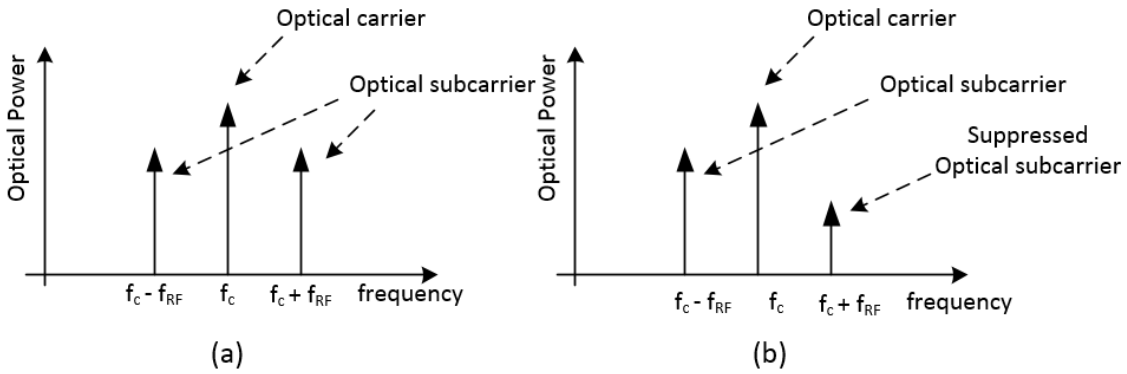

Figure 1-5 (a) DSB modulation and (b) SSB modulation.

1.2 Wireless signal formats

Using RoF links to transmit and distribute wireless signals, a lot of the signal distortions are caused by optical subcarrier modulations. However, other than the analog RoF transmission system, the distributed radio systems can be digitalized by using multi signal modulation formats such as quadrature amplitude modulation (QAM) and orthogonal frequency division multiplexing (OFDM). With the increasing demands of data rate and transmission bandwidth in wireless communication, OFDM is now considered the most promising approach by its capability of high data transmission rate and highly sufficient usage of bandwidth. Specifically, OFDM is a digital multi-carrier modulation scheme by using a large number of closely spaced orthogonal subcarriers to carry data, where each subcarrier is modulated by conventional modulation methods such as QAM and phase-shift keying (PSK). Popular OFDM based wireless signal formats include wireless local area network (WLAN) and ultra wideband (UWB).

1.2.1 Wireless local area network (WLAN) overview

WLAN is a local wireless communication method which links to two or more devices. The mobility and flexibility of this technology allow users to move freely in the coverage area, and WLANs have been widely deployed because of its easy to install feature and the trend of using mobile devices in recent years. IEEE 802.11 is the dominant standard in WLAN communications, and it is first released in 1997 as a set of specifications for computer communications at the frequency bands of 2.4 and 5 GHz. IEEE 802.11a and IEEE 802.11g are the two early protocols which were specifically assigned to use OFDM modulation. For IEEE 802.11g, the transmission channel consists of 52 sub-carriers where each subcarrier has a bandwidth of 312.5 KHz, then the subcarriers combined channel occupies 16.25 MHz bandwidth at the frequency of 2.4 GHz with the data rate up to 54 Mbits/s. In addition, every sub-carrier can use a unique modulation scheme. In the past few years, the above specifications are widely deployed to family internet routers and office WLAN implementation, and has made our life much more convenient than ever before.

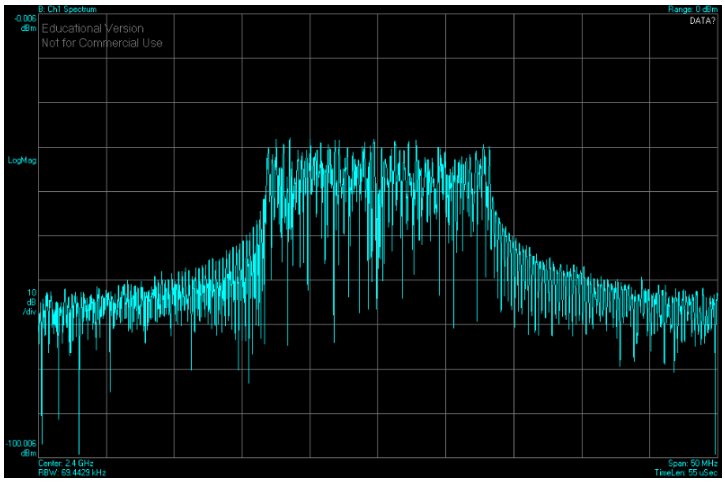

Figure 1-6 Spectrum of 802.11a WiFi signal.

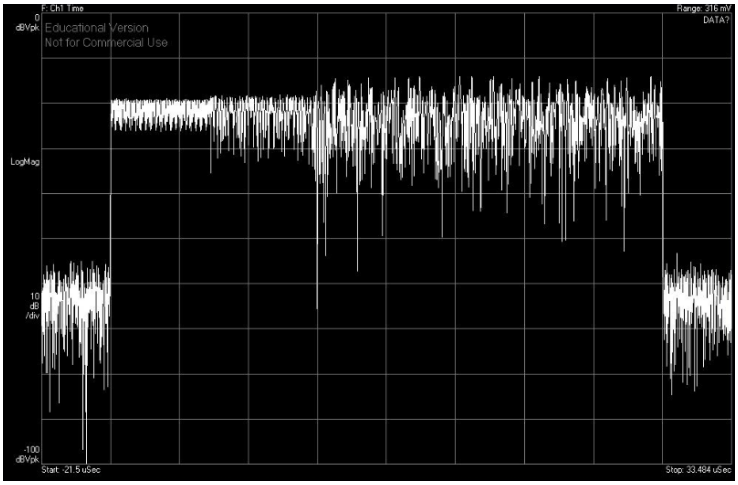

Figure 1-7 Time domain of 802.11a WiFi signal.

Figure1-6 shows the RF spectrum of 802.11a WiFi signal at the center frequency of 2.4 GHz with the data rate of 32 Mbits/s, and Figure 1-7 shows the time domain of 802.11a WiFi signal.

With the rapid development in this field, the IEEE 802.11n and IEEE 802.11ac were proposed in 2009 and 2013, respectively. Recently, Bell Canada deployed the IEEE 802.11ac protocol to their internet routers which support both 2.4 and 5 GHz frequency bands with the practical data rate up to 175 Mbits/s, and its fiber optic network where RoF technology can be applied has already replaced the traditional digital subscriber line (DSL) services.

1.2.2 Ultra wide band (UWB) overview

Nevertheless, people expect larger operational bandwidth and higher data rate. With its huge bandwidth (0.5 to 10.6 GHz), high data rate (55 to 480 Mbits/s) and low power spectral density, UWB is expected to have a major impact on next generation wireless communication such as 5G systems. In 2002, US Federal Communications Commission

(FCC) became the first to allocate the UWB application using the spectral band from 3.1 to 10.6 GHz with the less than -41.3 dBm/MHz transmitted power spectral density (PSD). Furthermore, the FCC defined UWB formats are specified to occupy an over 500 MHz frequency bandwidth, or its 10 dB bandwidth has at least 20% of the carrier frequency [11].

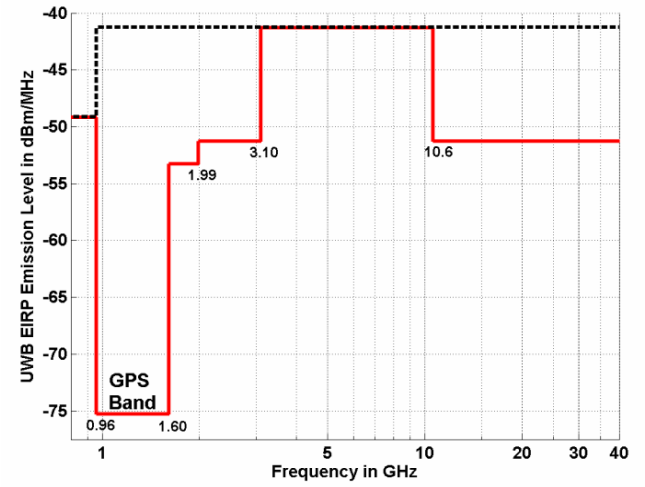

Figure 1-8 FCC indoor communication system emission level [11].

As shown in Figure 1-8, the FCC UWB operating range is from 3.1 to 10.6 GHz, but there is no specific regulation on the exact physical infrastructure. Therefore, several UWB techniques have been proposed such as direct sequence (DS-UWB) [11] and multiband orthogonal frequency division multiplexing (MB-OFDM).

The DS-UWB is a directly modulated single band approach which has a huge bandwidth of 7.5 GHz. As shown in Figure 1-9, MB-OFDM is a multiband modulation format which divides the entire 7.5 GHz bandwidth into 14 sub-bands, and these 14 sub-bands are being assigned to 6 large band groups [12]. Band group 1 to band group 5 consist of three sub-bands and there are two sub-bands in band group 6. Note that each sub-band contains 122 carriers that are spaced 4.125 MHz apart, then each sub-band occupies a total

bandwidth of 528 MHz. Only band group 1 is mandatory now, and the rest are reserved for the future.

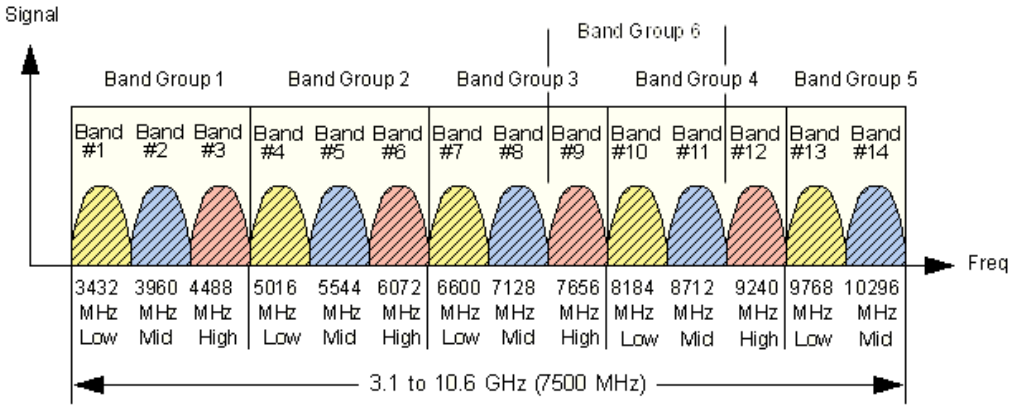

Figure 1-9 MB-OFDM UWB band groups [12].

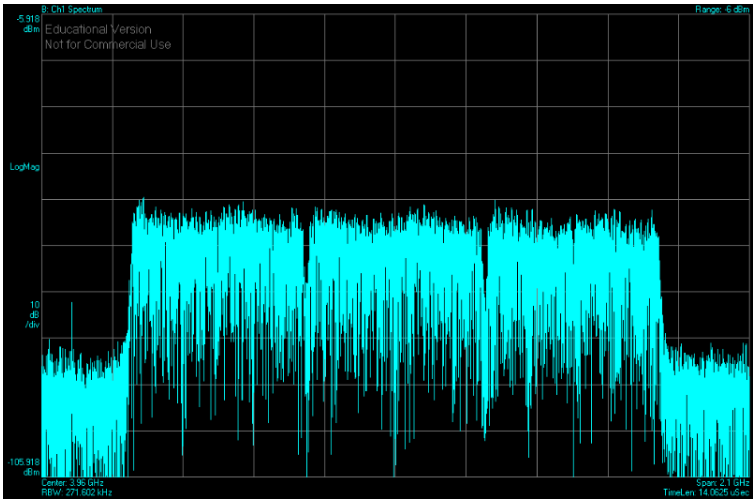

Figure 1-10 Spectrum of MB-OFDM UWB signal.

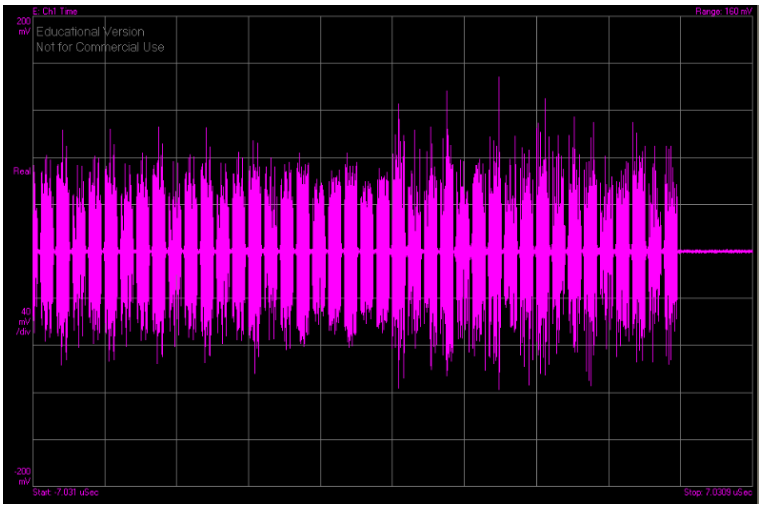

Figure 1-11 Time domain of MB-OFDM UWB signal.

Figure 1-10 shows the RF spectrum of three sub-bands in UWB band group 1 with the data rate of 200 Mbits/s. These three sub-bands are centered at the frequencies of 3.432, 3.96 and 4.488 GHz, respectively. The time domain of this UWB signal is shown in Figure 1-11.

As mentioned above, the UWB signal contains a low power spectral density feature, so propagating in the cable or in the free air will cost massive attenuation. Since one of the major limitations of WLAN is bandwidth, when a large amount of users are signed into the same WLAN communication system, the data transfer rate will be greatly reduced. However, optical fiber has the advantages of minimized loss, lower cost and large bandwidth, and thus it is very promising to use RoF transmission systems to transmit and distribute WLAN and UWB signals.

1.3 Nonlinearities of RoF transmission systems

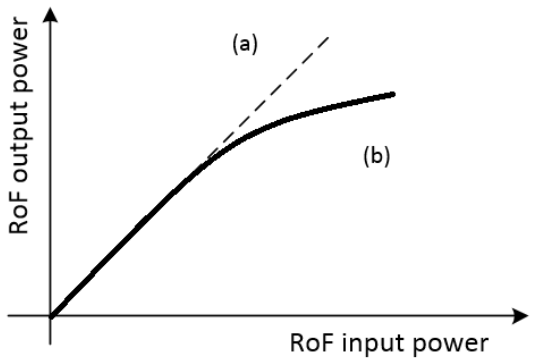

Figure 1-12 Schematic of (a) linear transmission and (b) nonlinear transmission of RoF systems.

In RoF transmission systems, the output power is expected to be linear to its input power which is shown in Figure 1-12 (a). However, the output of the system is always nonlinear to its input in practical transmissions. As shown in Figure 1-12 (b), as RoF input power increases, the RoF output power is not increasing as expected, which means the transmission of the RoF system is being suppressed. This introduces nonlinear distortions of RoF transmission systems. Fiber dispersion such as chromatic dispersion will be introduced by using optical fiber as the signal transmission media. In multimode fibers, modal dispersion (MD) introduces signal spread in time due to the different propagating velocities of optical signals, which are transmitting in different modes. However, for example, fiber dispersion generated by the transmission of wireless signals such as UWB and WiFi over a few kilometers single mode fiber (SMF), has very little influence on the nonlinearities of RoF transmission systems.

The major nonlinear distortion in RoF link is caused by the usage of RF components like RF power amplifiers (PAs) and optical components such as laser diodes, external electro-optical modulators, semiconductor optical amplifiers (SOAs) and photodiodes. The

nonlinear transfer functions of these devices result in harmonic distortion (HD) and intermodulation distortion (IMD). When considering single tone signal transmission in a RoF link, the output signal contains products at frequencies of integer multiples of the fundamental frequency which is shown in Figure 1-13, and this phenomenon is caused by HD.

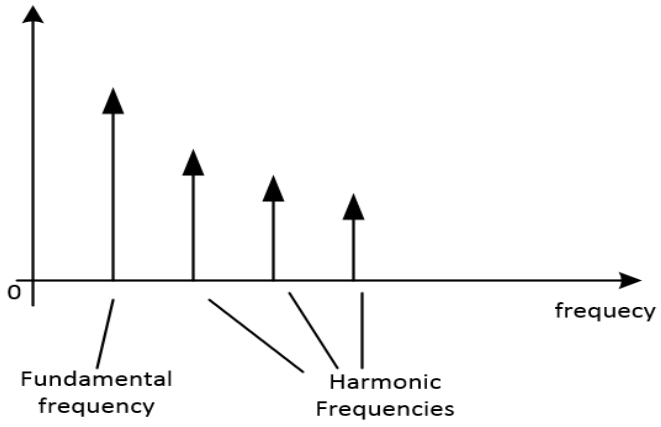

Figure 1-13 Harmonic distortion at RoF output.

IMD happens when two or more signals at adjacent frequencies are being transmitted in an RoF link, intermodulation between these signals generates more distortion products at frequencies other than harmonic frequencies. To analyze IMD mathematically, Taylor series as shown in equation (1.1) is used to model the nonlinearity of RoF transmission systems [13].

$$v_o = a_0 + a_1 v_i + a_2 {v_i}^2 + a_3 {v_i}^3 + \cdots, \tag{1.1}$$

where v_i and v_o are the input and output, respectively, and a denotes the coefficients. When the two tones of input signal are closly spaced at frequencies f_1 and f_2,

$$v_i = V_0(cos2\pi f_1 t + cos2\pi f_2 t) \tag{1.2}$$

Then from equation (1.1), the output of the RoF system can be derived as,

$$
\begin{aligned}
v_o &= a_0 + a_1V_0(cos2\pi f_1t + cos2\pi f_2t) + a_2V_0(cos2\pi f_1t + cos2\pi f_2t)^2 \\
&\quad + a_3V_0(cos2\pi f_1t + cos2\pi f_2t)^3 + \cdots \\
&= a_0 + a_1V_0cos2\pi f_1t + a_1V_0cos2\pi f_2t + \frac{1}{2}a_2{V_0}^2(1 + cos2\pi f_1t) \\
&\quad + \frac{1}{2}a_2{V_0}^2(1 + cos2\pi f_2t) + a_2{V_0}^2\cos(2\pi f_1 - 2\pi f_2)\,t \\
&\quad + a_2{V_0}^2\cos(2\pi f_1 + 2\pi f_2)\,t + a_3{V_0}^2\left(\frac{3}{4}cos2\pi f_1t + \frac{1}{4}cos6\pi f_1t\right) \\
&\quad + a_3{V_0}^2\left(\frac{3}{4}cos2\pi f_2t + \frac{1}{4}cos6\pi f_2t\right) + a_3{V_0}^2[\frac{3}{2}cos2\pi f_2t \\
&\quad + \frac{3}{4}\cos(4\pi f_1 - 2\pi f_2)\,t + \frac{3}{4}\cos(4\pi f_1 + 2\pi f_2)\,t] \\
&\quad + a_3{V_0}^2[\frac{3}{2}cos2\pi f_1t + \frac{3}{4}\cos(4\pi f_2 - 2\pi f_1)\,t \\
&\quad + \frac{3}{4}\cos(4\pi f_2 + 2\pi f_1)\,t]
\end{aligned}
\tag{1.3}
$$

The third order intermodulation (IMD3) products are at $2f_1 - f_2$, $2f_2 - f_1$, $2f_1 + f_2$and $2f_2 + f_1$ frequencies. $2f_1 - f_2$ and $2f_2 - f_1$ are located right next to the fundamental frequencies f_1 and f_2. Similarly, it is easy to derive from equation (1.1) that $3f_1 - 2f_2$ and $3f_2 - 2f_1$ are the two of fifth order intermodulation (IMD5) products that are closely located to fundamental frequencies. From equation (1.3), it is also possible to obtain the values of coefficients which represent the amplitudes of intermodulation products. The obtained amplitudes of IMD3 and IMD5 are related to their powers in RoF transmission. From Figure 1-14, it can be derived that second order intermodulation (IMD2) products have the largest powers among all IMD products, however IMD2s are located far from the fundamental frequencies. IMD3 has the second largest power among IMDs which is located in the transmission passband. IMD5 is also in the passband but with a lower power. Hence IMD3 should be considered the most important intermodulation product.

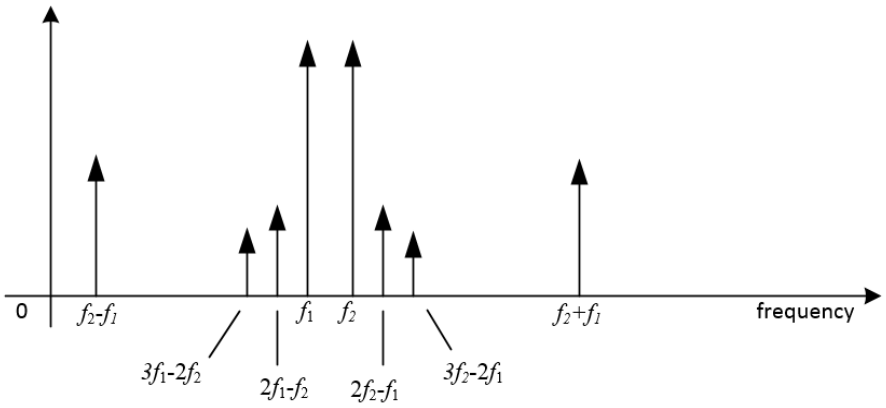

Figure 1-14 Schematic of the generated intermodulation products in nonlinear systems.

Note that, four wave mixing (FWM) is the most stand out optical nonlinear effect in RoF transmission systems. It is generated by the included optical components such as SOAs and optical modulators. As shown in Figure 1-15, two lights at the frequencies of f_1 and f_2 are generated by two CW lasers, respectively. Then, at the output of external optical modulator, two more lights at the frequencies of $2f_1 - f_2$and $2f_2 - f_1$ are generated. Thus it can be noticed that the FWM is an IMD phenomenon.

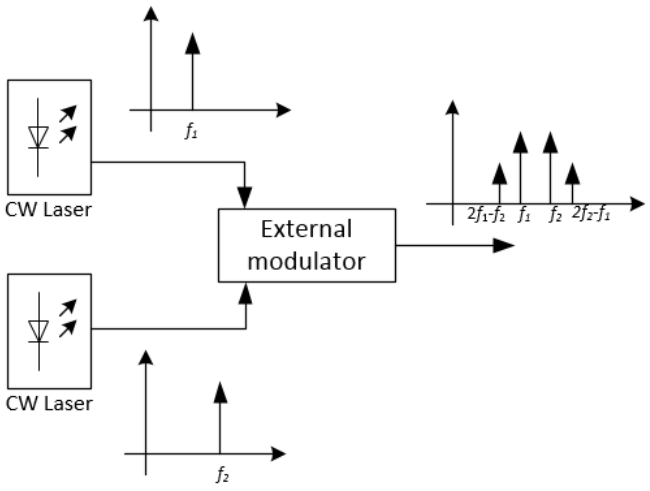

Figure 1-15 Schematic of four wave mixing (FWM) phenomenon.

It is possible to infer from equation (1-3) that odd order IMD products are formed closely to the fundamental frequencies which could be within the transmission passband. As shown in Figure 1-16, this kind of phenomenon is called 'spectrum regrowth'. Thus linearization techniques are highly needed in RoF links. As mentioned, the major causes of nonlinear distortions in RoF links are optical subcarrier modulation and RF power amplification, so most proposed techniques are targeted at these aspects.

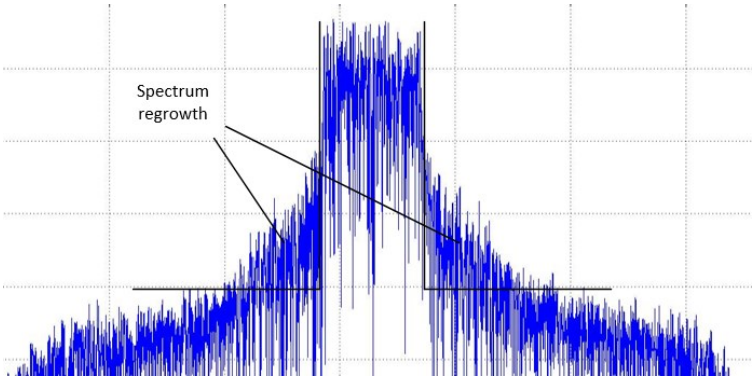

Figure 1-16 Spectrum regrowth.

1.4 Linearization techniques for RoF systems

Due to the nonlinearities of RoF links, various linearization techniques have been proposed within the past years. As shown in Figure 1-17, optical linearization and electrical linearization are the two principal approaches in the linearization for RoF transmission systems. Optical Linearization includes mixed-polarization [14-15], dual-wavelength [16] and etc, while electrical linearization includes analog predistortion circuit [17-19], digital predistortion (DPD) [20-26] and digital post-compensation (DPC) [27-30]. In predistortion, a spurious distortion is firstly generated and is applied to input of nonlinear systems, then the spurious distortion carried by the transmitted signal will suppress the nonlinear

distortion generated from RoF systems. The processing sequence of post-compensation is opposite to predistortion.

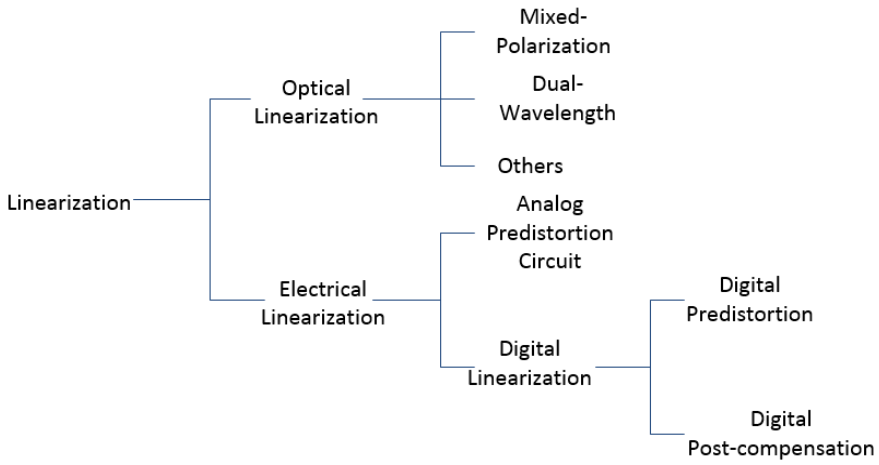

Figure 1-17 Linearization techniques [1].

1.4.1 Optical linearization

The principle of optical linearization is to use the two nonlinear products generated in RoF links to cancel each other while maintaining the linear products such as subcarrier carrying wireless signals. Mixed-polarization and dual-wavelength are the typical optical linearization methods for RoF links.

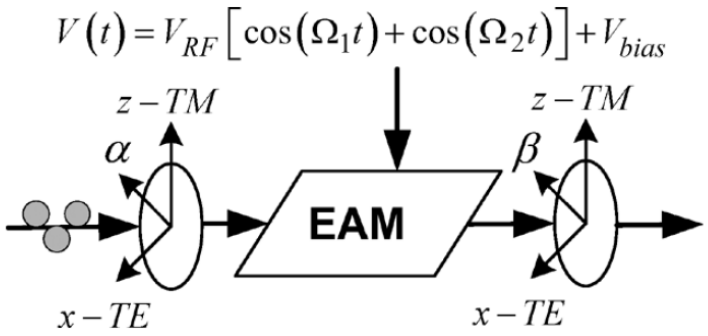

Figure 1-18 Schematic of mixed polarization EAM [14].

In [14], Hraimel et al. proposed and experimentally demonstrated optical mixed polarization technique for an EAM modulated RoF link. As shown in Figure 1-18, the

polarizers are, respectively, set to angle α and β with respect to z-axis. The light signal, which consists of the superposition of TE and TM optical field will be modulated by EAM first, then EAM output carries certain amounts of intermodulation products in its TE and TM optical fields. Because of the two angles in polarizers are carefully set which makes them related to each other, nonlinear distortion of the RoF system can be suppressed. In experimental demonstration, the mixed polarization EAM achieved a spurious-free dynamic range (SFDR) improvement of 8.1 and 9.5 dB in back to back and after 20 km fiber transmission.

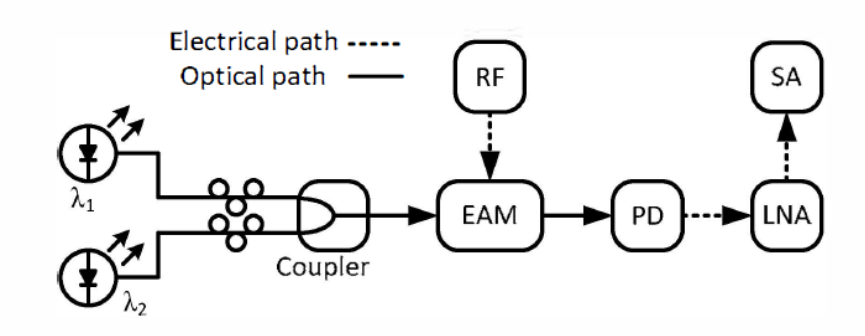

Figure 1-19 Schematic of dual-wavelength linearization [16].

Similarly, dual-wavelength method is using the nonlinear distortion products generated at different wavelengths λ_1 and λ_2 to cancel each other. In [16], Zhu et al. investigated linearization for RoF link with two lasers working at different wavelengths. As shown in Figure1-19, the wavelength of the two lasers are 1552.6 nm and 1510 nm, respectively. A C-band EAM is used as optical sub-carrier modulator. By carefully setting the power ratio of the two lasers, the nonlinearities from both lasers can be set antiphase. In this way, nonlinear distortions of both lasers are expected to be suppressed. The experimental results show that both HD2 and HD3 can be suppressed by 23 and 2.1 dB, respectively.

The optical linearization is considered as the predistortion method which can suppress both odd and even orders nonlinearities, and the suppression of nonlinearity covers the whole RF modulation bandwidth of the external modulator.

1.4.2 Analog predistortion circuit

Analog predistortion circuit is a typical technique in electrical RoF linearization. The principle of analog predisortion circuit is shown in Figure1-20, IMD3 is the suppression target in the diagram. The optical modulator in OTx for electrical to optical (E/O) conversion is modulating two signals adjacently centered at f_1 and f_2. The upper part of Figure 1-20 shows the intermodulation products introduced by IMD3 at $2f_1 - f_2$ and $2f_2 - f_1$. When applying analog predistortion circuit which is shown in the lower part of the figure, the antiphase IMD3 products which generated from the analog predistortion circuit will cancel the IMD3 products generated from RoF link. In this way, the suppression of IMD3 is realized.

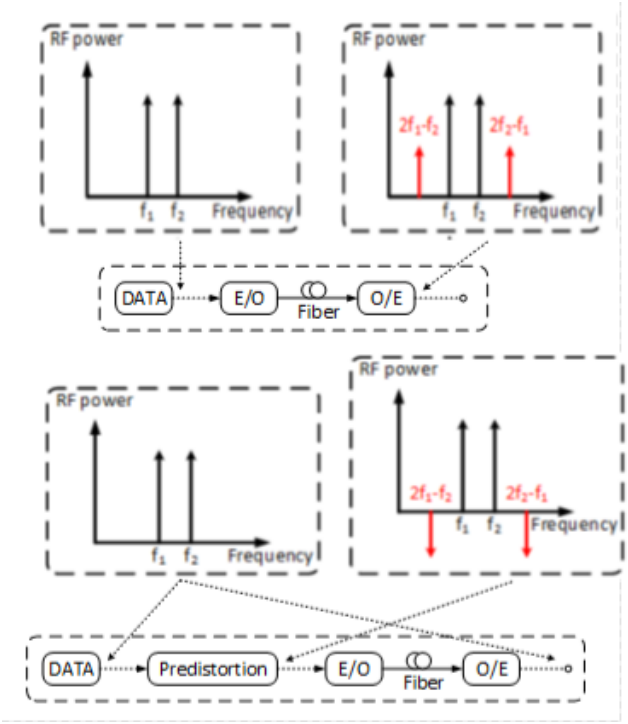

Figure 1-20 Principle of *analog predistortion circuit* linearization technique [1].

Using analog predistortion circuit to linearize RoF transmission systems, the conventional configurations of the circuits are shown in Figure1-21. The input signal has been split into two propagating paths, the lower path goes through the predistortion unit, and the upper path got time delay. At the output end of the circuit, a power combiner is used to combine the two paths.

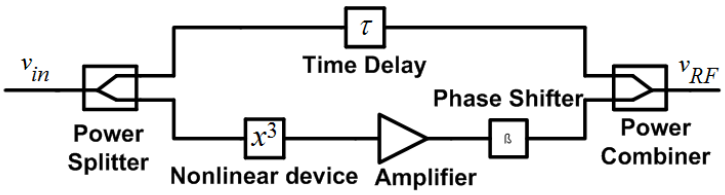

Figure 1-21 Predistortion circuit block [18].

In [17], Zhu et al. designed a low cost broadband predistortion circuit. As shown in Figure 1-22, the circuit uses two Wilkinson power dividers (WPDs) to split and combine

the transmitted signal. Two GaAs beam lead detector diodes at zero bias are used to generate the predistortion signals. In the experiment, the circuit is applied to remove the IMD3 of an EAM based RoF system. Around 9 dB improvement of spurious-free dynamic range (SFDR) from 7 to 14 GHz, and around 4 dB improvement of SFDR from 15 to 18 GHz were achieved.

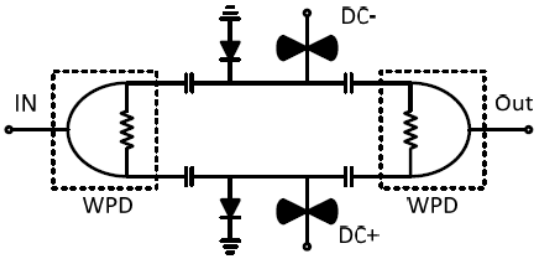

Figure 1-22 Schematic of broadband predistortion circuit [17].

Shen et al. proposed and experimentally demonstrated a simple analog predistortion circuit as shown in Figure 1-23 [18]. The power splitter splits the input signal into two transmission paths, and odd order nonlinear distortion products are generated after the signals have gone through the two antiparallel diodes. The applied quarter wave transformers are used for impedance matching. In the circuit, neither phase shifters nor amplifiers are used. In the experiment, the circuit is implemented for the linearization of MB-OFDM RoF transmission system. The verification results show a more than 7 dB suppression of IMD3 and 11 dB improvement in SFDR over 1.7 GHz transmission bandwidth.

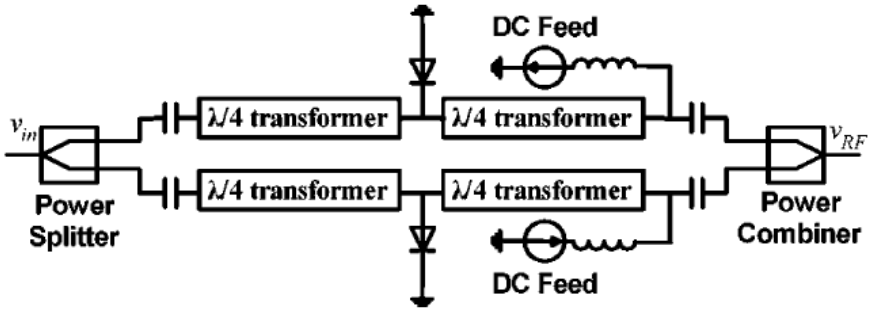

Figure 1-23 Reflective antiparallel diodes based analog predistortion circuit [18].

In [19], Zhu et al. designed a broadband analog predistortion circuit to suppress IMD3 which is generated from an RoF transmission system. The analog predistortion circuit is shown in Figure 1-24, consisting of a dual Schottky diode and broadband resistors. And broadband capacitors and inductors are applied as bias tees. Only one direct current (DC) source is used to bias the dual Schottky diode. To evaluate the performance of the circuit, EAM is used for optical subcarrier modulation in an RoF system. More than 10 dB improvement in SFDR from 1 to 5 GHz was achieved.

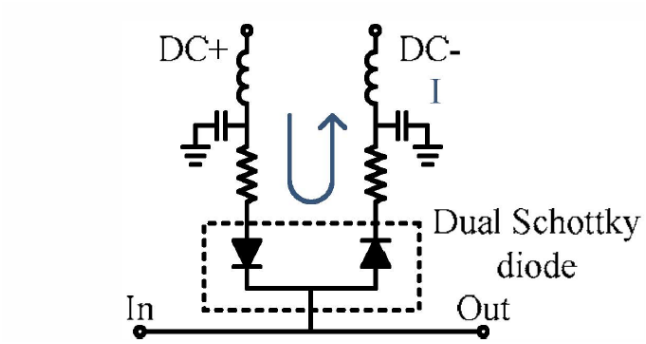

Figure 1-24 Schematic of broadband analog predistortion circuit circuit [19].

Analog predistortion circuit method is economically friendly because the analog components are cheap, and by integrating all components in a signal circuit, the compact size of the circuit benefits the allocation of this technology. However, it can be found out from the above circuits, all the components are fixed on the circuit board, so it is hard to

control phase and amplitude in analog circuit linearization techniques. Besides, the amplifiers used in the analog circuit might generate new nonlinear distortion and mix it with the original nonlinearities. Furthermore, analog circuit technology cannot provide enough linearization because it cannot suppress even order nonlinearities in broadband RoF transmissions.

Digital linearization is another technique among electrical RoF linearization approaches, which provides higher accuracy and better improvement. The detailed explanation of digital linearization will be presented in the next chapter.

1.5 Thesis outline

The rest of the thesis is organised as follows,

Chapter 2 discussed the digital linearization techniques for RoF links and RF power amplifiers. DPD and DPC are the two approaches in digital linearization. After reviewing the techniques of recent years. Research goals are proposed.

Chapter 3 theoretically analyzed the nonlinear distortions of RoF links, and the nonlinearities of RoF transmission system are modeled. To train the digital predistorter, the extraction of predistorter coefficients is explained and performed.

Chapter 4 presents the DPD verifications for RoF links in the experiments, and the DPD for WiFi over fiber transmission systems is implemented and verified. The same adaptive DPD technique for WiFi and MB-OFDM UWB over fiber transmission systems is verified as well.

Chapter 5 concludes the works that have been accomplished in the thesis and suggests the future works.

Chapter 2 Digital Linearization

2.1 Digital linearization techniques

As we discussed, DPD and DPC are the two approaches of digital linearization for RoF transmission systems. In digital linearization, an analog to digital converter (ADC) is used to sample the transmitted signals, then linearization is achieved by digital signal processing (DSP), where the opposite nonlinear distortion products are generated to compensate or post-compensate for nonlinearity generated from RoF transmission. Among all linearization techniques, digital linearization is the most flexible and accurate approach.

The schematic of DPC technique is shown in Figure 2-1: at the output of RoF link, a postdistorter is applied to compensate for the nonlinear distortion generated in RoF transmission. To extract the coefficients of postdistorter, monitoring of the received signal is needed. Coefficients of postdistorter are obtained when desired output signal is acquired. In DPC, the training of the postdistorter requires data analysis based on multiple cycles of the output signal sweep which limits processing speed and efficiency.

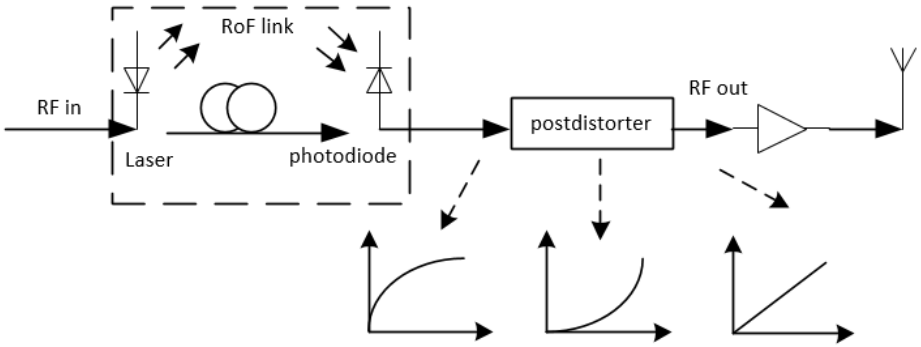

Figure 2-1 Schematic of DPC technique.

Compared to DPC, DPD technique can be more straight-forward and provide better results. Certain equations are applied to model the nonlinear RoF transmission systems. The schematic of DPD is shown in Figure 2-2, which contains the procedures: first step is to apply the signal data which is extracted from RoF input and output in an algorithm, second step is to calculate the coefficients of predisorter, the last step is to use the predistorter to generate spurious distortion products. x and y are the extracted input and output of RoF transmission system, y/g is the predistorter input where g denotes the gain of RoF system, then the output of predistorter training block x' can be obtained from the modeling equation of the RoF system, and coefficients of the predistorter training block are extracted by applying an estimation algorithm to minimize the difference $e = |x' - x|$. By using the obtained coefficients, it is able to generate the spurious distortion by the trained predistorter. Note that in broadband RoF transmissions, the output signal might not only be related to the simultaneous input signal, but is also affected by the previous inputs. Memory model in the DPD is then studied with respect to nonlinearity and memory effect of RoF systems. The predistorter can be adaptive for various transmission signal formats and broadband RoF links. By directly processing the input and output signal data of RoF systems, DPD is much more flexible and efficient than any other linearization techniques.

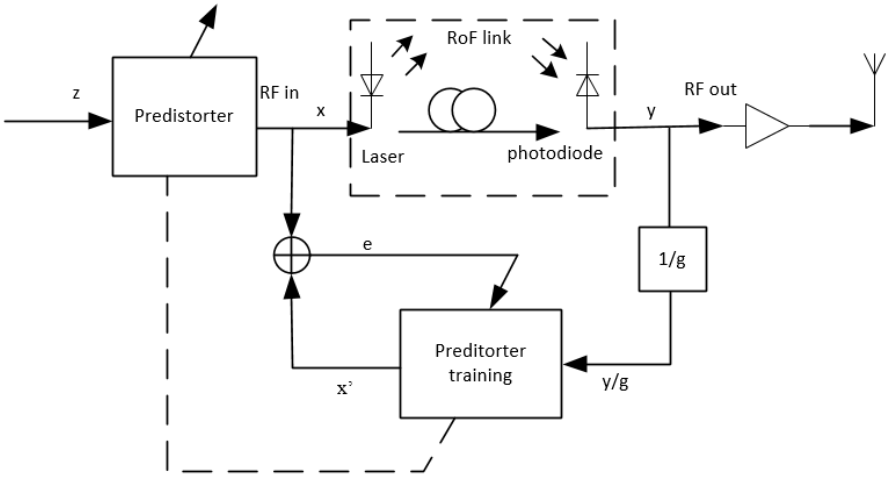

Figure 2-2 Schematic of DPD technique.

2.2 Literature review

As the discussed linearization techniques for RoF transmission systems, the optical methods are able to realize linearization for ultra-broad transmission bandwidth. However, they are more complex than analog predistortion circuit and optical components are hard to integrate. Analog predistortion circuits are cheap and simple, but even order nonlinearities are almost impossible to be suppressed. Due to these issues, digital linearization which includes DPD and DPC approaches provides better solutions. Note that DPD was firstly proposed to linearize RF power amplifiers (PAs) [31-39]. After many years of investigations on DPD and the alike nonlinearities, DPD is then applied in linearization for RoF transmission systems.

2.2.1 DPD for RF power amplifiers

The early proposed DPD techniques focused on linearizing memoryless RF power amplifiers (PAs). By using pulse shaping filters, the predistortion can be directly applied to the constellation points of input signal. However, the transmission bandwidth of memoryless PAs is limited.

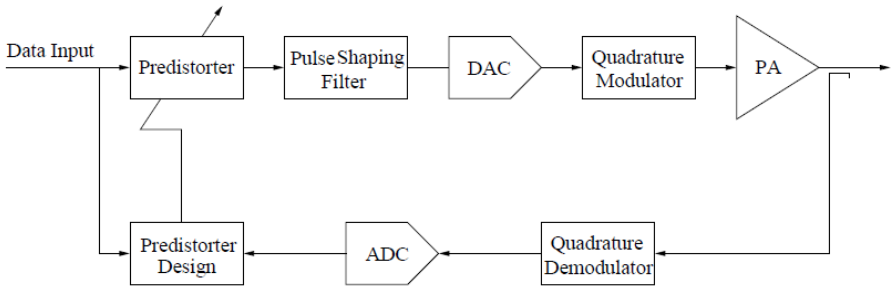

Figure 2-3 Schematic diagram of data predistortion for RF power amplifiers [35].

In [35], Karam et al. proposed a data predistortion technique to compensate for nonlinearities of a high power amplifier. As shown in Figure 2-3, a pulse shaping filter is located right after the predistorter. The pulse shaping filter generates values of input signal at three data points per symbol interval. Nonlinear distortion of the PA is reduced by predistorting each data point. The simulation shows that an up to 3.5 dB gain was achieved. Similarly, the RF bandpass filter in Figure 2-4 is used as the pulse shaping filter [36]. Then using the same technique, the predistorter is capable to compensate for the nonlinearities of PAs.

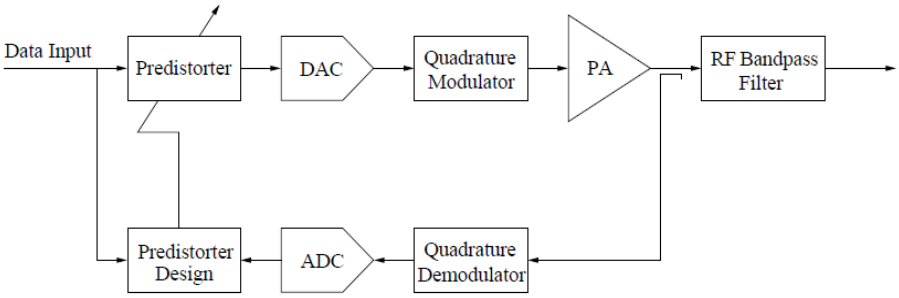

Figure 2-4 Schematic diagram of digital predistortion linearizer [36].

PAs of wideband RF transmission systems usually contain memory effects. Then theoretical modeling of PAs needs to include both nonlinear distortions and the memory effect. As shown in Figure 2-5, a couple of models have been proposed. Wiener model

which includes a linear time-invariant (LTI) system and a memoryless module (NL), is used by Clark et al. for wideband PA modeling [37]. Compared to conventional memoryless model, Wiener model provides a better accuracy in PA modeling. Kang et al. used DPD based on Hammerstein model to compensate for nonlinear distortions of an OFDM system [38]. However, the predistorter had limited performance. The Wiener-Hammerstein model is shown in Figure 2-5 (c), LTI system is followed by a NL which is followed by another LTI. Wiener-Hammerstein model is usually used to model amplifiers of satellite communication channels [39].

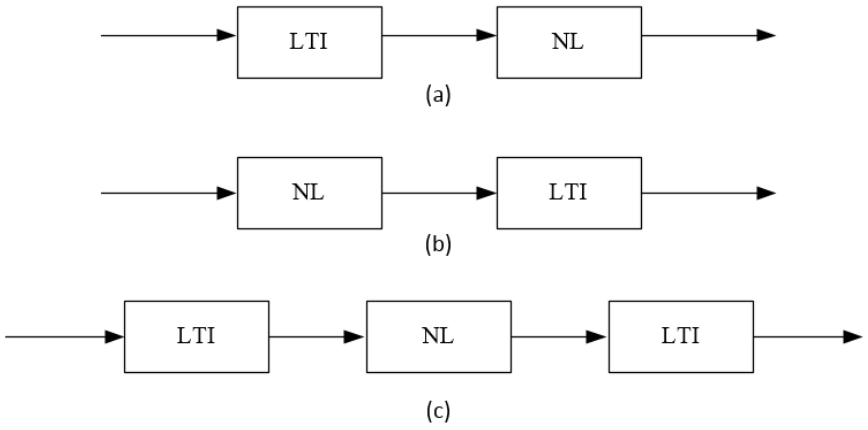

Figure 2-5 Model nonlinearities of power amplifiers with memory effect: (a) Wiener model (b) Hammerstein model (c) Wiener-Hammerstein model.

In [31], Ding et al. proposed the memory model which describes the nonlinearities and memory effect of PAs. Simulation results show that odd order nonlinearities are slightly suppressed by implementing DPD which is based on early memoryless model. Whereas odd order nonlinearities are almost completely suppressed by performing DPD based on memory model. Using similar methods to linearize a system with a transmission bandwidth of 20 MHz, an around 10 dB improvement of EVM was achieved [32-33].

To perform DPD for PA with a larger transmission bandwidth, Hammi et al. proposed a DPD technique based on a cascade model as shown in Figure 2-6. The proposed model is similar to Wiener model [34]. The experiment results show that nonlinearity can be suppressed over 300 MHz transmission bandwidth. However, the proposed DPD technique suffers from a serious drawback which is the lack of computational efficiency.

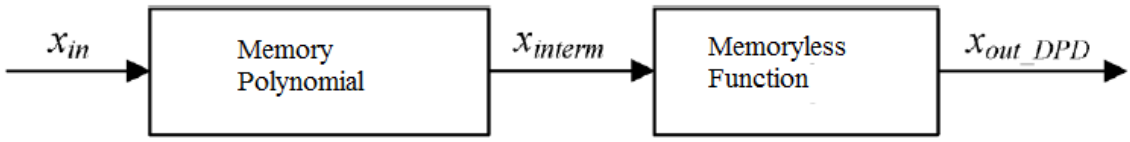

Figure 2-6 Model nonlinearities of power amplifiers: Cascade model [34].

2.2.2 Digital linearization for RoF transmission systems

RoF transmission systems include RF power amplifiers (PAs), so the nonlinearities of RoF transmission systems include the nonlinearity generated by PAs. Digital linearization techniques are therefore investigated and applied in linearization for RoF systems. As discussed in section 2.1, DPC and DPD are the two major research fields of digital linearization for RoF transmission systems.

Lee et al. proposed a postdistortion compensation technique [27]. The proposed postdistorter is allocated at the output of RoF system. According to the nonlinear characteristics of RoF systems, a related inverse function is loaded in the postdistorter. So after the distorted signal goes through the inverse function, nonlinearities are expected to be suppressed. Simulation results show that a 10 dB improvement of DR is realized. However, other than simulation, a more persuasive demonstration is not given.

Pei et al. proposed a digital multichannel post linearization technique [28] to linearize broadband RoF transmission systems and considering the analog to digital conversion limitations. As shown in Figure 2-7, a multi-band RF signal is transmitted through RoF system. The post compensation is then performed at the output of RoF after frequency down conversion. The experimental results show a more than 3 dB improvement of DR of a two-band RoF link. Since the nonlinearity of the RoF is unknown, it has to recursively sweep the output signal of RoF system, to monitor the adjacent channel power (ACP) to extract the postdistorter coefficients. The recursive sweeping decreases the linearization efficiency. Besides, every channel in the transmission system needs to extract its own coefficients, which increases the computational complexity.

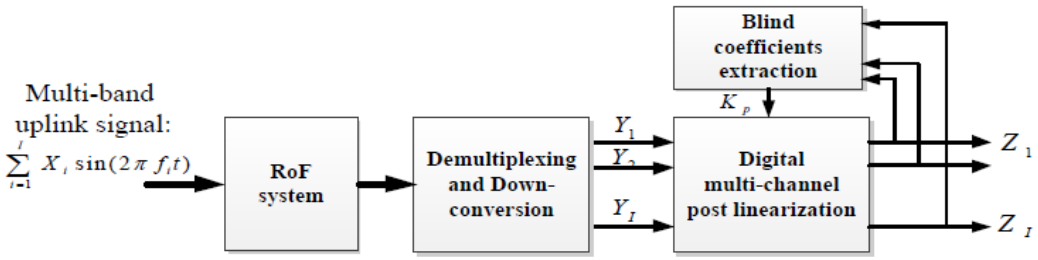

Figure 2-7 Digital multi-channel post linearization technique [28].

DPD is another digital linearization approach, compared to postdistortion compensation, it is more straight forward and precise. Other than applying inverse function or blind learning the nonlinearity of the applied RoF system, it directly uses an algorithm where the RoF system's input and output signal data are applied to train a predistorter. Reversed nonlinear products are then generated in predistorter before the signal is transmitted into the RoF system.

Due to memory effects, the memoryless polynomial is not sufficient to model broadband RoF transmission systems. The memory polynomial is then applied to model

the RoF transmission. Vieria et al. used a scheme which is shown in Figure 2-8 to study a behavioral model [20]. RoF system is transmitting a signal at 1 GHz with 20 MHz bandwidth. By putting the complex baseband RoF input and output signals into the Agilent Distortion Suite software, coefficients are estimated and applied directly to the predistorter. It was shown that a 10 dB better accuracy of normalized mean square error (NMSE) was achieved in the proposed DPD than in previous memoryless model based DPD. However, DPD is applied in a narrowband transmission system, so the demonstration of DPD for broadband RoF transmission system is required to be verified.

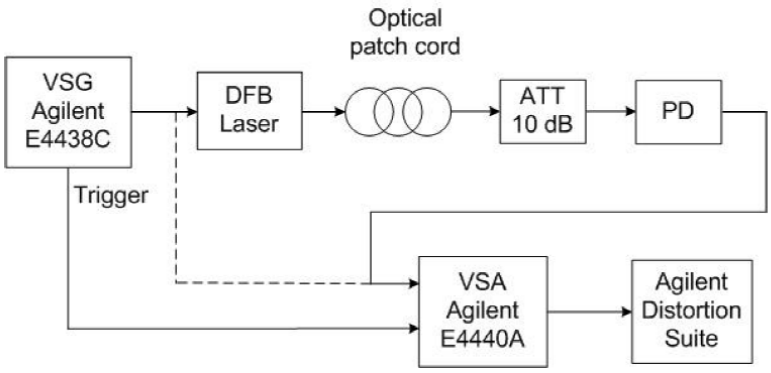

Figure 2-8 Behavioral modeling DPD [20].

Similar to the earlier mentioned DPC techniques, in order to improve the performance of linearization for broadband RoF transmission systems, Chen et al. proposed a DPD technique for multi-channel RoF link [21]. As shown in Figure 2-9, two baseband signals are generated separately from two devices and up converted to 2.3 and 2.462 GHz, then the combined signal is transmitted through optical link. To estimate the coefficients, an offline signal processing in Matlab using the input baseband signal data and down converted output signal data is carried out. In the end, linearization for multi-channel RoF is realized in this research, and experimental results show an around 12 dB error vector

magnitude (EVM) improvement. However, the calculation efficiency of the coefficients estimation from complex baseband signal is low. The number of coefficients increases dramatically as more channels are added into the system.

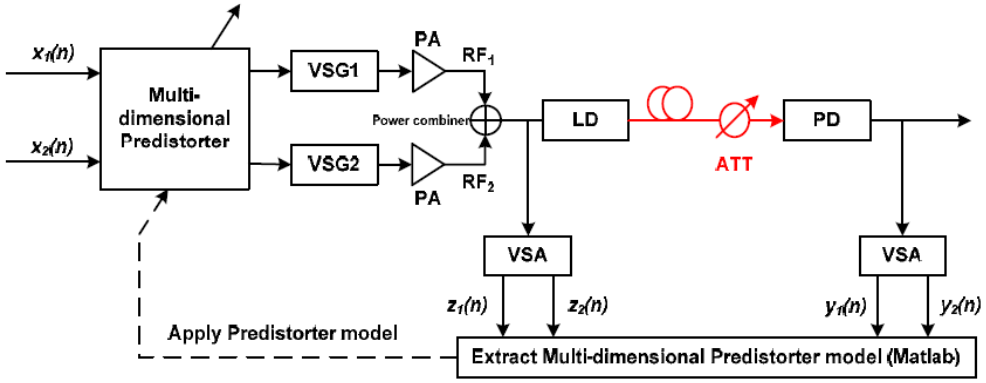

Figure 2-9 Multi-band digital predistortion [21].

Omomukuyo proposed an architecture to linearize MB-OFDM ultra wideband (UWB) over fiber system [22]. Compared to [20] [21], the MB-OFDM signal with a large bandwidth is transmitting in a RoF system. A 9 dB improvement of EVM has been achieved in the experiment. However, the implemented DPD was targeted at only one sub-band of 528 MHz centered at 3.432 GHz from FCC UWB band group 1, and extraction of coefficients is lack of efficiency. Among all reviewed DPD technologies, extra frequency up and down conversions are needed since predistorters are placed at baseband, this reduces the speed of calculation. Besides, signals with different formats will be transmitted simultaneously in actual RoF systems. Thus, DPD technique with better efficiency for linearization of broadband RoF systems is required to be investigated.

2.3 Research motivations

This research is focused on designing a DPD technique with highly computational efficiency for broadband RoF transmission systems. WiFi signal at 2.4 GHz and whole band group 1 of FCC UWB signal at 3.96 GHz are applied in this work.

In order to achieve good computational efficiency, unlike most of the digital predistortion techniques of using complex baseband signal data, this DPD technique is implemented in RF domain. There is no extra frequency up and down conversion procedures in the verifications. The proposed DPD technique is applied to linearize the directly modulated RoF transmission systems. The implemented DPD is targeted at the broad transmission bandwidth of over 2.4 GHz.

Chapter 3 Theoretical Analysis of Digital Predistortion

RoF transmission systems are popularly used to transmit and distribute RF signals over long distance for broad operational bandwidth and low attenuation advantages. To sufficiently use the broad bandwidth, deployment of multiple signals in RoF transmission such as WLAN, worldwide interoperability for microwave access (WiMAX) and ultra wide band (UWB) signals, is preferred. And all of RoF links exhibit some nonlinear behaviors due to the nonlinear transfer functions of the included optical and RF components. Linearization is thus important in RoF system implementations. Among all linearization techniques over RoF links, the digital linearization is the most effective way to suppress the nonlinear distortion of RoF links. Digital Predistortion (DPD) is a typical digital linearization approach which is more adaptive and precise. The adaptive DPD is a technique which is regardless of the modulation formats of transmitted signals. To achieve this adaptive feature, an adaptive algorithm is needed in the DPD. As discussed, the training of predistorter is required in the DPD implementation. The first step in training is to apply RoF input and output data reversely to the predistorter block as its output and input. Note that the predistorter block is modeled by a nonlinear transfer function. The second step is to use an algorithm to estimate the coefficients of predistorter. After acquiring the coefficients, the last step is to apply the trained predistorter directly to the RoF input to generate the opposite nonlinear products. As thus, it is expected that the suppression of nonlinear distortion of RoF transmission systems is obtained. In this chapter, the order of sections is following the above sequence to discuss and analyze the proposed DPD technique.

3.1 Modeling nonlinearities of RoF systems

As mentioned earlier, the major problems of transmitting wireless signals in an RoF link are the generation of nonlinear distortion. If the nonlinear system is transmitting a single tone signal, only harmonic distortion (HD) will be generated. At the output of the nonlinear system, some signals with frequencies of integer multiple of the fundamental frequency will be received. While there are two or more tones signals transmitting in the nonlinear system, both HD and intermodulation distortion (IMD) will be generated. As multi-carrier signal formats are widely used in RoF links, compared to HD, IMD is more of the metric which determines nonlinear degrees of an RoF transmission system. Both RF nonlinearity and optical nonlinearity will be generated in RoF transmission. Since the major optical nonlinearity (four wave mixing) is similar to IMD of RF nonlinearity in principle, mathematical modeling nonlinearities of RoF transmission systems will be carried out in RF domain.

Figure 3-1 Nonlinear RoF system.

The nonlinear RoF system that has the input $x(n)$ and output $z(n)$ as shown in Figure 3-1 can be generally modeled based on the Taylor series in (1.1) [13],

$$z(n) = a_0 + a_1x(n) + a_2x(n)^2 + a_3x(n)^3 + a_4x(n)^4 + a_5x(n)^5 \ldots, \qquad (3.1)$$

In Taylor series, only instant relation between system input and output is considered. Then, we can model a nonlinear system by eliciting the memoryless polynomial from

equation (3.1), where $x(n)$ and $z(n)$ are system input and output, respectively. a_k denotes the coefficients of the nonlinear system ($k \geq 1$).

$$z(n) = \sum_{k=1}^{K} a_k x(n) \tag{3.2}$$

However, in broadband RoF transmission systems, the system output may not only be related to the instantaneous input, but is also related to previous inputs. This phenomenon is referred as the memory effect. Thus in order to model the nonlinearity of RoF systems with memory effects, it is required to add memory variables into the existing memoryless polynomial, Volterra series [40] is then used which describes nonlinearities of RoF systems by considering both nonlinear distortion and the memory effect. Volterra series is similar to Taylor series but has the ability to describe memory effects, from equation (3.2), by adding memory variable $'m'$,

$$a_k x(n) = \sum_{m_1=0}^{M-1}, \dots, \sum_{m_k=0}^{M-1} h_k(m_1, \dots, m_k) \prod_{l=1}^{K} x(n - m_k) \tag{3.3}$$

where h_k is called Volterra kernels, and m denotes the memory depth which indicates how many system inputs are related to the system output. And in RoF transmission systems, the memory depth $m \geq 0$, nonlinear order $l = 1,2,3, \dots, k-1$, then we can apply (3.3) to (3.2), we have,

$$z(n) = \sum_{k=1}^{K} \sum_{m_1=0}^{M} \sum_{m_2=1}^{M}, \dots, \sum_{m_k=k-1}^{M} h_k(m_1, \dots, m_k) \prod_{k=1}^{K} x(n - m_k) \tag{3.4}$$

where K and M denote nonlinear order and memory depth, respectively. Since Volterra series contains a lot of coefficients. So in extraction of coefficients, Volterra series might not be able to provide a good computational efficiency. Memory Polynomial [41] in

equation (3.5) is a simplified case to model the nonlinearities of RoF systems when considering memory effects.

$$z(n) = \sum_{p=1}^{P} \sum_{q=0}^{Q} k_{pq} x(n-q)|x(n-q)|^{p-1} \tag{3.5}$$

where p is nonlinear order, q is memory length, k_{pq} is the coefficient of predistorter which is related to both nonlinear order and memory depth. Also, the memory polynomial considers both even and odd order nonlinearities. In this thesis, this memory polynomial is directly used to model the nonlinearities of WiFi and UWB over fiber transmission systems. And to obtain highly computational efficiency, other than applying complex baseband signal data in the polynomial, RF signal is directly used in the extraction of coefficients. In the upcoming section, the explanation of highly computational efficiency will be presented.

3.2 Extraction of model coefficients

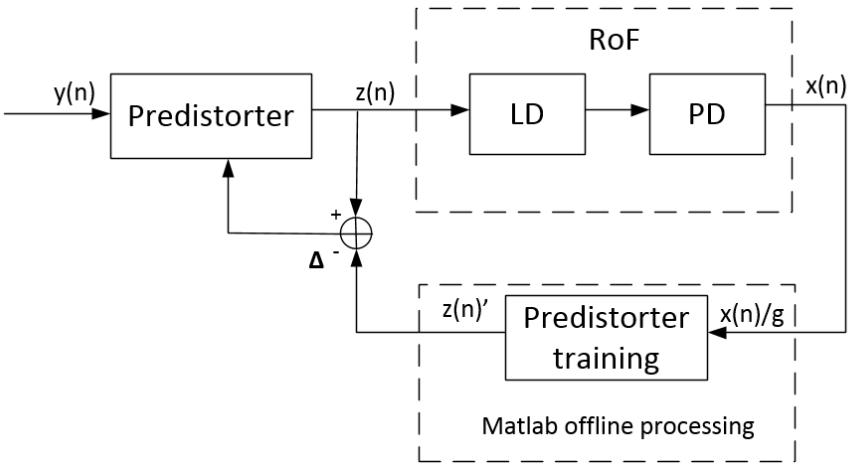

Figure 3-2 Schematic of predistorter training block.

After modeling the nonlinear broadband RoF transmission system, it is required to train a digital predistorter by extracting its coefficients as shown in Figure 3-2. As the predistorter training block is modeled by (3.5), the corresponding equation for this case is,

$$z(n)' = \sum_{p=1}^{P} \sum_{q=0}^{Q} k_{pq} \frac{x(n-q)}{g} \left| \frac{x(n-q)}{g} \right|^{p-1} \tag{3.6}$$

where $x(n-q)/g$ and $z(n)'$ are the input and output of the predistorter, respectively. g denotes the gain of the RoF system.

3.2.1 Least square (LS) method

In DSP process of the DPD, it is required to sample the transmitted signal, then use the data to extract coefficients of the predistorter. Due to the sample by sample feature of the sampled digital signals, least square (LS) method is a good approach for its fast convergence rate when limited variables are applied in the estimation of coefficients. The proposed model requires exactly this kind of computational efficiency and accuracy. Thus, LS method is considered the most appropriate approach in estimation of coefficients. As shown in Figure 3-2, to calculate the coefficients, LS method is used to minimize the square errors which is the difference between predistorter output $z(n)'$ and RoF input $z(n)$.

In equation (3.6), if we define that,

$$u_{pq} = \frac{x(n-q)}{g} \left| \frac{x(n-q)}{g} \right|^{p-1} \tag{3.7}$$

then we can derive a simple relation between predistorter output and coefficients by applying (3.7) into (3.6),

$$Z = KU \tag{3.8}$$

where,

$$\begin{aligned} Z &= [z(0), z(1), \dots, z(n)]^T \\ K &= \left[k_{10}, \dots, k_{p0}, \dots, k_{1q}, \dots, k_{pq}\right]^T \end{aligned} \tag{3.9}$$

$$U = [u_{10}, \dots, u_{p0}, \dots, u_{1q}, \dots, u_{pq}]$$

$$u_{pq} = [u_{pq}(0), u_{pq}(1), \dots, u_{pq}(n)]^T$$

$[.]^T$ denotes matrix transpose. The elements in matrixes Z and U are related to the input and output of the predistorter. And the number of the elements in both matrixes depends on the actual samples that are used in the extraction of coefficients. The subscripts p and q denote nonlinear order and memory depth, respectively. Since the RoF transmission system input and output signal data are already sampled, LS method is applied to acquire the matrix K which contains the coefficients elements. The idea of applying LS method in the proposed model is shown in Figure 3-3, the input $\sum Z(i)$ and output $\sum X(i)$ of RoF transmission link are obtained firstly. Then, the input of the predistorter is acquired by using the output divided by the gain g of RoF transmission link which results in $\sum X(i)/g$. And from equation (3.6), $\sum Z(i)'$is the predistorter output.

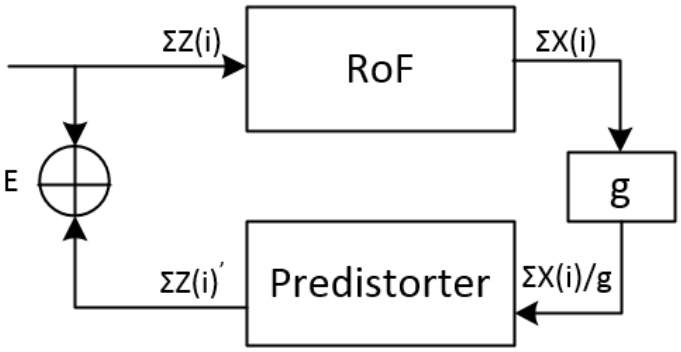

Figure 3-3 Schematic of LS method in extraction of coefficients.

In estimation of coefficients, it is expected to minimize the squared error E which describes the difference between $\sum Z(i)$ and $\sum Z(i)'$, given by,

$$E = \sum_{i=1}^{i=n} (Z_i - KX_i)^2 \tag{3.10}$$

where $Z_i$and X_i contain the system input and output data, respectively. From equation (3.6), $\sum KX_i$ is expression of the output $\sum Z(i)'$ of the predistorter, and $i = n$ denotes that there are n signal samples being calculated in the estimation of coefficients. To minimize the error E, the following condition must be satisfied,

$$\frac{\partial E}{\partial K} = 0 \tag{3.11}$$

Then by taking partial derivative of (3.10), we obtain (3.12),

$$\sum_{i=1}^{i=n} \big(2 \times (KX_i - Z_i)\big) X_i = 0 \tag{3.12}$$

In the broadband RoF transmission system, high sampling rate is needed in sampling the broadband carrier. Then the offline DSP in Matlab is going to process the massive signal data. Thus, it is tended to operate the LS estimation in matrix form as defined in (3.9). By solving (3.12) with the processed data in matrix form, we can derive the solution for extraction of coefficients which is shown in (3.13),

$$K = (U^T U)^{-1} U^T \mathrm{Z} \tag{3.13}$$

where $(.)^T$ denotes matrix transpose, and matrixes U and Z contain elements which are related to the extracted input and output signal data of the RoF transmission system. K is the $N \times 1$ matrix, where the included elements are the coefficients of predistorter.

3.2.2 Experimental extraction of model coefficients: a case

As discussed in the above section, we modeled the predistorter and derived the solution of LS method for the extraction of coefficients. Then, in this section, a specific extraction of coefficients in experiment is introduced. In DPD technique, both nonlinear orders and

memory effect are considered. The number of coefficients increases when higher nonlinear order and more memory depths are included in the extraction of coefficients, and number of coefficients is related to the time which is required in the extraction of coefficients. Besides, LS method has the high accuracy advantage under the limited variables involved circumstance.

Thus, by considering the above reasons, a case is presented as an example: up to third order nonlinearities and two memory depths. When applying nonlinear order $p = 3$ and memory depth $q = 2$ in equation (3.6), we can derive the elements of matrix U from equation (3.9) as shown in Table 3-1

Table 3-1 Memory polynomial model expansion

Coefficients (k_{pq})	Matrix U	Coefficients (k_{pq})	Matrix U
k_{10}	$u_{10} = \frac{x(n)}{g}$	k_{31}	$u_{31} = \frac{x(n-1)}{g}\left\lvert\frac{x(n-1)}{g}\right\rvert^{2}$
k_{20}	$u_{20} = \frac{x(n)}{g}\left\lvert\frac{x(n)}{g}\right\rvert$	k_{12}	$u_{12} = \frac{x(n-2)}{g}$
k_{30}	$u_{30} = \frac{x(n)}{g}\left\lvert\frac{x(n)}{g}\right\rvert^{2}$	k_{22}	$u_{22} = \frac{x(n-2)}{g}\left\lvert\frac{x(n-2)}{g}\right\rvert$
k_{11}	$u_{11} = \frac{x(n-1)}{g}$	k_{32}	$u_{32} = \frac{x(n-2)}{g}\left\lvert\frac{x(n-2)}{g}\right\rvert^{2}$
k_{21}	$u_{21} = \frac{x(n-1)}{g}\left\lvert\frac{x(n-1)}{g}\right\rvert$		

From Table 3-1, it is seen that the elements in matrix U are listed, then every element value can be determined from the sampled data of the predistorter input $x(n)$. In experiment, $x(n)$ data and system gain g can be acquired from the output of RoF transmission system.

Note that each u_{pq} also represents a $n \times 1$ matrix whose size is dependent on the number of samples n, for example,

$$u_{10} = [u_{10}(1), u_{10}(2), \dots, u_{10}(n)\ ]^T \tag{3.14}$$

As seen in Table 3-1, the matrix U in this case is expressed as,

$$U = [u_{10}, u_{20}, u_{30}, u_{11}, u_{21}, u_{31}, u_{12}, u_{22}, u_{32}] \tag{3.15}$$

Also, from equation (3.9), matrix Z contains the predistorter output signal data which can be acquired from the input of RoF transmission system. Z has the same matrix size as u_{pq}.

The final step is to apply these matrixes in LS method solution (3.13). Matrix K which contains predistorter coefficients is then obtained as,

$$K = [k_{10}, k_{20}, k_{30}, k_{11}, k_{21}, k_{31}, k_{12}, k_{22}, k_{32},\ ]^T \tag{3.16}$$

As shown in (3.16), nine coefficients are calculated in the extraction of coefficients when considering up to third order nonlinearities and the memory depth of two. Then it is easy to infer that fifteen coefficients should be calculated when considering up to fifth order nonlinearities and memory depth of two. In this situation, an extra 67% of calculation time is added. Similarly, when longer memory depth is considered, the calculation time will be added relatively. So the number of coefficients is the most important criteria which influences the computational efficiency and processing rate of the proposed DPD technique. In the considered method, compared to the extraction of coefficients shown in [23], only half number of the coefficients are calculated for an RoF system modeled using the same nonlinear order and memory depth. Table 3-2 presents the number of coefficients associated with nonlinear order and memory depth of the proposed DPD for RoF transmission systems.

Table 3-2 Number of coefficients in DPD

Nonlinear order	Memory depth	Number of coefficients
Up to third	0	3
Up to third	1	6
Up to third	2	9
Up to fifth	0	5
Up to fifth	1	10
Up to fifth	2	15

3.3 Summary

At this point, the calculation method of coefficients in DPD technique has been presented and analyzed step by step. The obtained coefficients can be directly applied to the predistorter. We can then apply the trained predistorter in linearization of an RoF transmission system as shown in Figure 3-4.

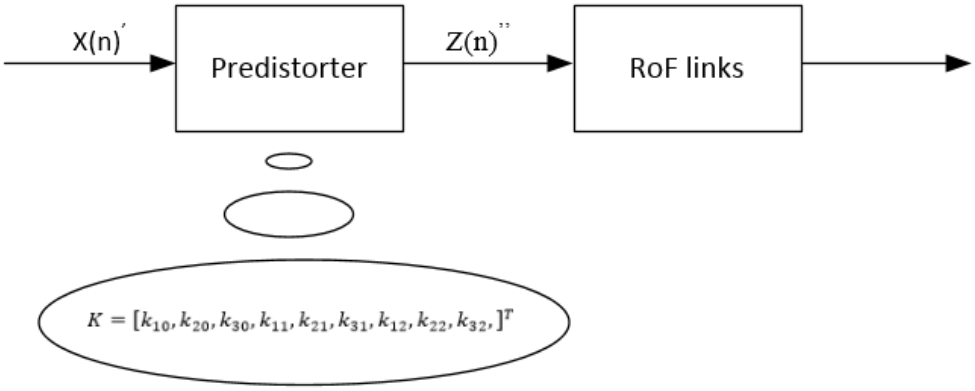

Figure 3-4 Implementation of DPD technique.

The predistorter follows equation (3.5) and also contains the transmission coefficients as shown in matrix K. After applying the predistorter to the input of RoF links, the predistorted RoF transmission system input $Z(n)''$ which contains opposite nonlinear

distortion products can be easily obtained. So far, DPD process for RoF transmission systems is finished and RoF systems nonlinearity are expected to be suppressed.

In the next chapter, DPD technique will be implemented and verified experimentally. Besides, multiple signals with various modulation schemes will be transmitted simultaneously in real broadband RoF transmission systems. So other than applying DPD technique to linearize RoF systems which are transmitting one signal, a DPD for RoF systems which are transmitting two signals will be implemented and tested in the upcoming chapter.

Chapter 4 DPD Verifications in RoF Transmission Systems

In this chapter, the adaptive DPD technique is verified experimentally. To evaluate the performance of the DPD for broadband RoF transmission systems, two experiments are carried out. The first one is DPD for WiFi over fiber transmission system. The WiFi signal is centered at 2.4 GHz. The second one is DPD for WiFi and UWB over fiber system. The WiFi and UWB signals are centered at 2.4 GHz and 3.96 GHz, respectively. In the experiments, scenarios of both back to back (BTB) and 10 km single mode fiber (SMF) transmission are included. The measured error vector magnitudes (EVMs) of the RoF transmission system outputs without and with the DPD are given to evaluate the performance.

4.1 Experimental setup with related characterization instruments

In the predistorter training of DPD, it is required to extract the sampled signal data from input and output of RoF transmission systems. Usually, data extraction is realized by signal generators and signal analyzers. Thus, these instruments are crucial to the calculation and evaluation of DPD.

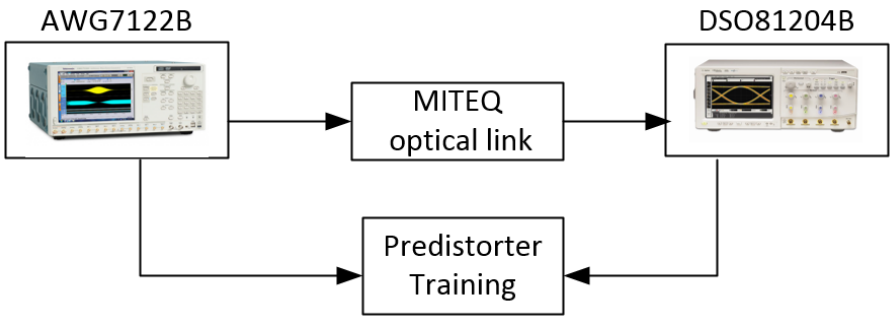

Figure 4-1 Signal generator and analyzer in RoF digital predistortion

In the experiments, firstly, we need to generate an RF signal as the input of the RoF links. Arbitrary Waveform Generator (AWG) and Vector Signal Generator (VSG) are the two most commonly used instruments in signal generation. In this work, a Tektronix AWG7122B is used to generate the inputs of the RoF links. AWG7122B has a maximum sampling rate of 24 GSa/s which supports the effective RF output frequency up to 9.6 GHz. The embedded RFXpress software (RFX100) fully exploits the wideband signal generation capacities of AWG7122B by supporting a wide range of signal modulation formats. For example, MB-OFDM UWB signal which occupies over 1.5 GHz bandwidth can be defined and modified in RFX100.

At the RoF output, Vector Signal Analyzer (VSA) is needed to analyze the received signal. In this thesis. Agilent real-time oscilloscope DSO81204B is applied to extract RoF output data. DSO81204B has the maximum sampling rate of 40 GSa/s which supports the receivable frequency up to 12 GHz. Then the embedded software VSA89600 in DSO81204B is used to acquire EVM to mark the quality of the received signal.

In the experiments, the proposed DPD is verified in directly modulated RoF transmission systems. The experimental setup is given in Figure 4-1. A MITEQ SCM fiber optical link (MITEQ-SCML-100M6G) which has a 3 dB bandwidth of 6 GHz is used in the RoF transmission systems. The block diagram of the MITEQ link is shown in Figure 4-2. A laser with 1550 nm wavelength is integrated in the optical transmitter (OTx) for optical subcarrier modulation. An optical signal with the power of 5 mW is then transmitted to the optical receiver (ORx). For optical to electrical (O/E) conversion, the modulated optical signal at 1550 nm wavelength is detected and demodulated by a photodiode with the responsivity of 0.6 A/W. Two direct current (DC) power supplies are used to bias the

OTx and ORx. Also as shown in Figure 4-2, a low noise amplifier (LNA) and a transimpedance amplifier are integrated in both the OTx and ORx, respectively. The related gain of the link is 18 dB. Besides, 1 m SMF (BTB) and a 10 km SMF are used to connect the OTx to ORx, respectively. The applied SMF has an optical attenuation of 0.28 dB/km.

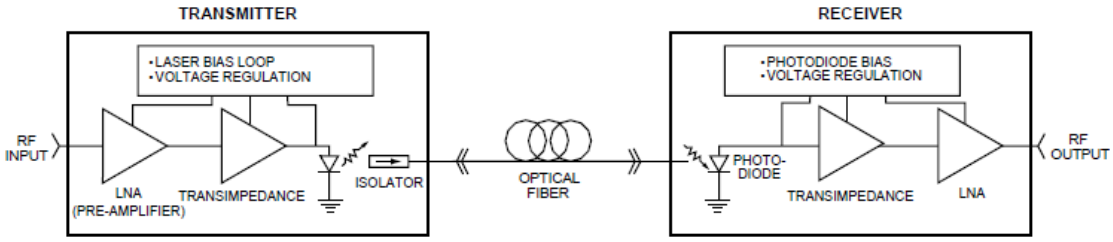

Figure 4-2 MITEQ optical transmitter and receiver [42]

4.2 DPD verifications in WiFi over fiber systems

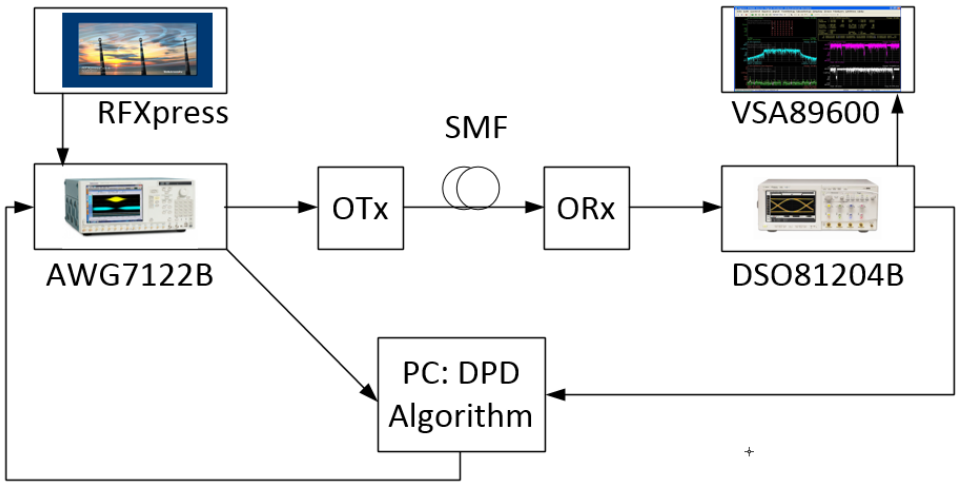

Figure 4-3 Experimental configuration of the DPD for WiFi over fiber systems

The experimental configuration is shown in Figure 4-3. Tektronics AWG7122B and RFXpress software are used to generate a WiFi signal as the input of RoF system. The WiFi signal follows IEEE 802.11a protocol at the center frequency of 2.4 GHz. The data rate is 36 Mbit/s and 16 QAM modulation scheme is used. By using 52 subcarriers OFDM modulation format, in which the subcarrier spacing is 312.5 KHz, the created WiFi signal occupies 20 MHz bandwidth. Two scenarios are included in the optical signal transmission: one is by connecting OTx to ORx with 1 m SMF, i.e., BTB, and the other is by connecting OTx to ORx with 10 km SMF. DSO81204B and VSA89600 are used to capture and analyze RoF output signal. After extracting the sampled RF input and output signals from AWG7122B and DSO81204B, respectively, a Matlab offline processing in a PC is performed to extract the coefficients and generate predistorted signal. As discussed at the end of Chapter 3, the predistorted signal will be fed into AWG7122B, and then sent to the RoF transmission system. The linearization performance is evaluated by comparing the EVM of the received signals before and after applying DPD for WiFi over fiber

transmission systems. The EVM can be acquired in VSA89600 software of DSO81204B oscilloscope.

4.2.1 DPD verification in back to back WiFi over fiber system

Table 4-1 Extracted coefficients of the predistorter for BTB WiFi over fiber system

Up to third order nonlinearities	$k_{10} = 0.8929$
	$k_{20} = -0.2291$
	$k_{30} = 0.7248$
Up to fifth order nonlinearities	$k_{10} = 0.8324$
	$k_{20} = 0.3194$
	$k_{30} = -0.6919$
	$k_{40} = 1.0433$
	$k_{50} = 0.0863$

Firstly, the DPD for BTB WiFi over fiber transmission system is verified. Two cases are considered: up to third order and fifth order nonlinearities. Coefficients of the predistorter are calculated and shown in Table 4-1. The DPD performance is analyzed in BTB WiFi over fiber transmission system. As shown in Figure 4-4, the measured EVM versus input RF power is given for three cases: without the DPD and the DPD for up to third and fifth order nonlinearities. After the DPD is applied, the measured EVMs are decreased with the input RF power. However, the improvements of the EVMs are reduced when the system input power is too low. In other words, the performance of the DPD is dependent on the input RF power, and the DPD provides the best performance at the input power of -18.5 dBm, where the EVM is improved from -23.7 dB to -31.9 dB, i.e., an improvement of 8.2 dB. However, the increase of nonlinear order from third to fifth does not leads to better improvement in linearization. The possible reason could be that the

power of the fifth order nonlinearity is much lower compared to the third order nonlinearity. The third order nonlinearity is the dominant nonlinear component in this directly modulated WiFi over fiber system.

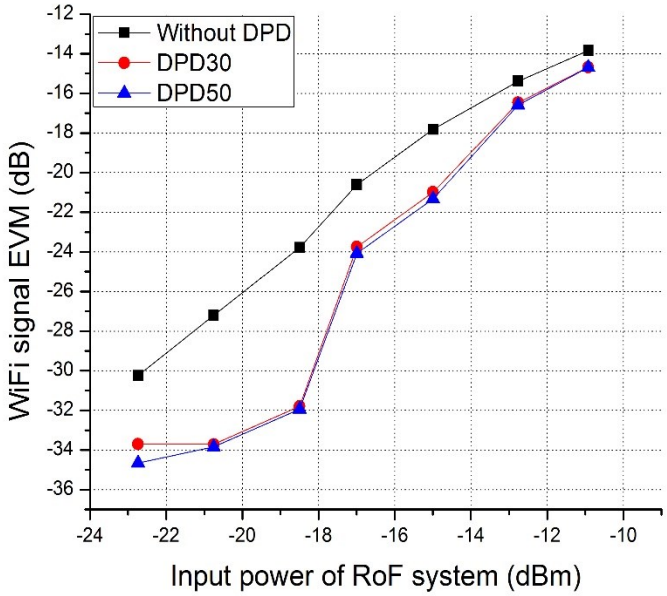

Figure 4-4 Measured EVM at output of BTB WiFi over fiber system. DPD30: up to third order nonlinearities. DPD50: up to fifth order nonlinearities

The constellation diagram of the transmitted WiFi signal, i.e., 16 QAM at the system output is shown in Figure 4-5. At the input RF power of -18.5 dBm, by using the DPD for up to fifth order nonlinearities, constellation diagram is improved since the signal is more concentrated.

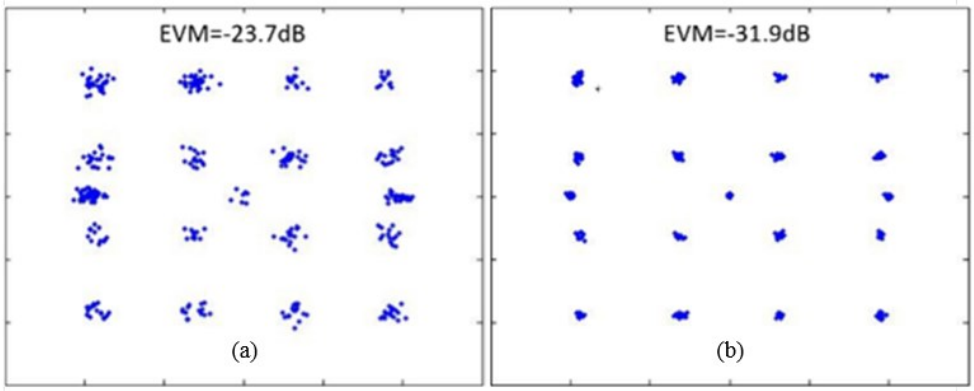

Figure 4-5 Measured constellation diagrams of the output signals in BTB WiFi over fiber system (a) without and (b) with the DPD for up to fifth order nonlinearities

Secondly, when memory effects are included, the extracted coefficients of the two cases are given in Table 4-2, i.e., the DPD for up to third order and fifth order nonlinearities with memory depth of zero, one and two. Better improvements are achieved by considering higher order nonlinearity and more memory effect. As shown in Figure 4-6, the measured EVM versus the input RF power is illustrated in seven cases: without the DPD, the DPD for up to third order nonlinearities, the DPD for up to third order nonlinearities with memory depth of one, the DPD for up to third order nonlinearities with memory depth of two, the DPD for up to fifth order nonlinearities, the DPD for up to fifth order nonlinearities with memory depth of one and the DPD for up to fifth order nonlinearities with memory depth of two. At the input RF power of -16.9 dBm, the DPD for up to third order nonlinearities with the memory depth of zero results in an EVM improvement from -20.6 dB to -23.7 dB, i.e., 3.1 dB. However, by using the DPD for up to fifth order nonlinearities with the memory depth of two, the EVM improvement becomes from -20.6 dB to -26.6 dB, i.e., 6 dB. It is seen that, the EVM is improved by up to 3 dB when the memory effect is considered for the input RF power of -16.9 dBm and -20.9 dBm. However, there is no

improvement of EVM at other input RF power. It can be seen that the memory effect in the directly modulated RoF transmission system is input RF power-sensitive.

Table 4-2 Extracted coefficients of the predistorter for BTB WiFi over fiber system

Memory depth	$q = 0$	$q = 1$	$q = 2$
Up to third order nonlinearities	k_{10} = 0.8430	k_{11} = 0.6099	k_{12} = -0.0435
	k_{20} = -0.3348	k_{21} = -0.4055	k_{22} = -0.2556
	k_{30} = 0.7214	k_{31} = 0.9504	k_{32} = 0.6634
Up to fifth order nonlinearities	k_{10} = 0.7140	k_{11} = 0.4597	k_{12} = -0.0435
	k_{20} = 1.2030	k_{21} = 0.8248	k_{22} = -0.0044
	k_{30} = -5.1732	k_{31} = -1.9746	k_{32} = 2.3064
	k_{40} = 9.0086	k_{41} = 2.1179	k_{42} = -5.9338
	k_{50} = -4.7513	k_{51} = -0.0297	k_{52} = 4.7118

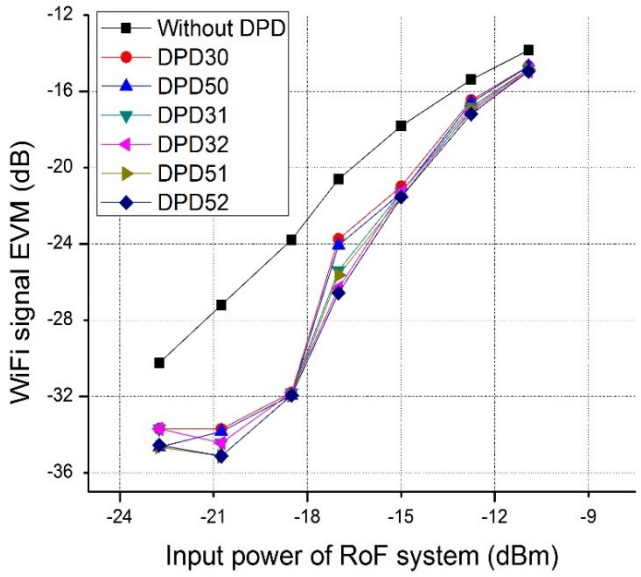

Figure 4-6 Measured EVMs at output of WiFi BTB RoF transmission system. DPD30: up to third order nonlinearities. DPD31: up to third order nonlinearities with one memory depth. DPD32: up to third order nonlinearities with two memory depths. DPD50: up to fifth order nonlinearities. DPD51: up to fifth order nonlinearities with one memory depth. DPD52: up to fifth order nonlinearities with two memory depths.

As shown in Figure 4-7, the constellation diagrams of the transmitted WiFi signal, i.e., 16 QAM at the system output are compared. By using the DPD for up to fifth order nonlinearities with memory depth of two, the constellation diagram is clearly improved at the input RF power of -16.9 dBm. The improvement of EVM from -20.6 dB to -26.6 dB, i.e., 6 dB is achieved.

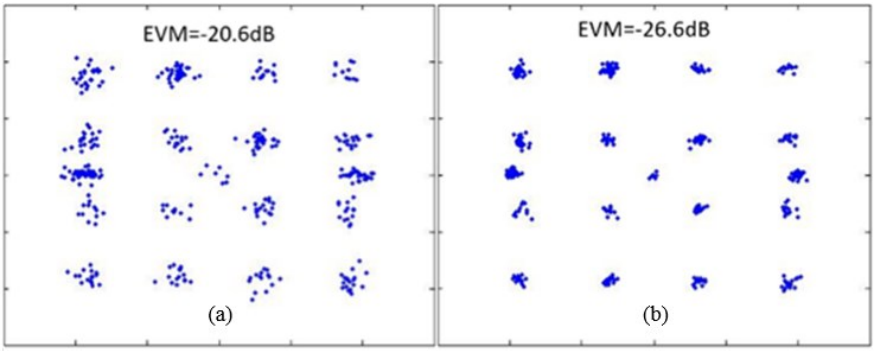

Figure 4-7 Measured constellation diagrams of the output signals in BTB WiFi over fiber system (a) without and (b) with the DPD for up to fifth order nonlinearities with two memory depths

4.2.2 DPD verification in WiFi over 10 km SMF transmission system

Table 4-3. Extracted coefficients of the predistorter for WiFi over 10 SMF transmission system

Up to third order nonlinearities	$k_{10} = -0.6339$
	$k_{20} = -0.1522$
	$k_{30} = -0.0401$
Up to fifth order nonlinearities	$k_{10} = -0.4859$
	$k_{20} = -1.9801$
	$k_{30} = 7.0582$
	$k_{40} = -10.8169$
	$k_{50} = 5.6170$

To verify the DPD for WiFi over 10 km SMF transmission system, Still, two cases are considered: up to third order and fifth order nonlinearities. The extracted coefficients of the predistorter for the above cases are given in Table 4-3. The DPD performance is analyzed in the WiFi over 10 km SMF, as shown in Figure 4-8, in which the measured EVM versus the input RF power is given in three cases: without the DPD, the DPD for up to third order nonlinearities and the DPD for up to fifth order nonlinearities. Again, the improvement by the DPD is dependent on the input RF power, and the DPD results in the best improvement at -16.5 dBm, where the EVM is improved from -21.6 dB to -27.2 dB,

i.e., a 5.6 dB improvement. At the input power of -16.5 dBm and -19.5 dBm, the EVMs are improved when considering fifth order nonlinearity. However, there is no additional improvement at other input power when considering fifth order nonlinearity. The reason is that the power of the fifth order nonlinearity achieves the minimum for the input RF power of –17.5 and -18.5 dBm. And the fifth order nonlinearity is saturated when the input RF power is higher than -15.5 dBm.

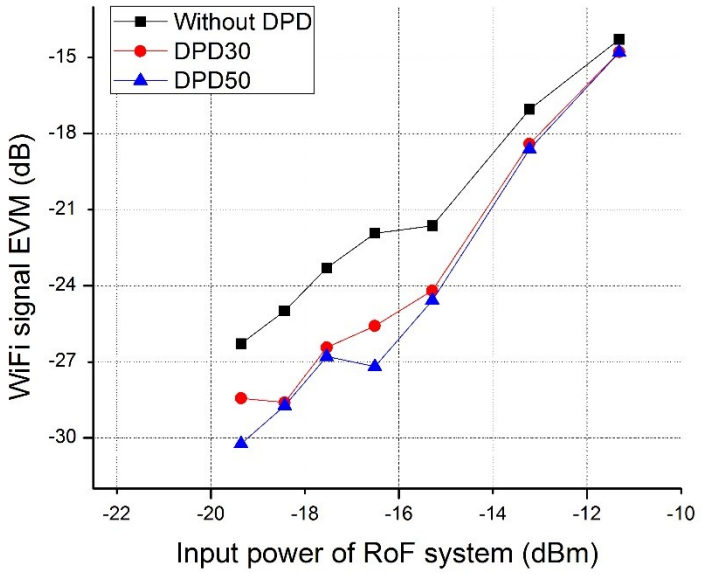

Figure 4-8 Measured EVMs at the output of WiFi over 10 km SMF transmission system. DPD30: up to third order nonlinearities. DPD50: up to fifth order nonlinearities.

To clearly show the improvement achieved by the DPD, we also measure the signal constellation diagrams of the transmitted signals, i.e., 16QAM, at the system output. For using the DPD for up to fifth order nonlinearities, the constellation diagrams at the input RF power of -16.5 dBm are compared in Figure 4-9, clearly illustrating the improvement of signal integrity.

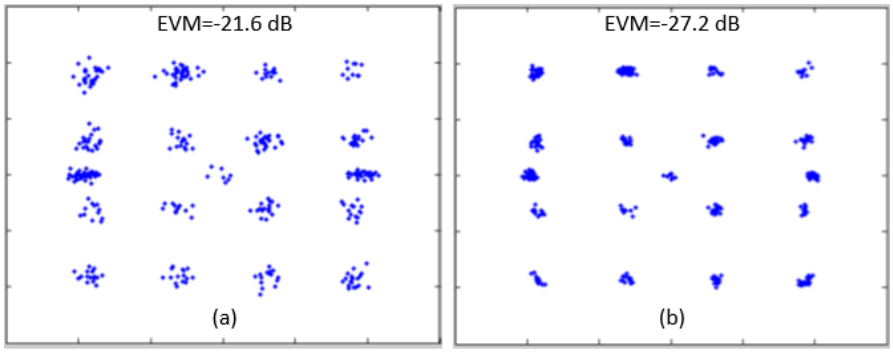

Figure 4-9 Measured constellation diagrams at the output of WiFi over 10 km SMF transmission system (a) without and (b) with the DPD for up to fifth order nonlinearities

Similarly, when the memory effect is included, the extracted coefficients for the two cases are given in Table 4-4, i.e., the DPD for up to third order nonlinearities and for up to fifth order nonlinearities. By considering higher order nonlinearity and memory effect, better improvements are achieved as shown in Figure 4-10, in which the measured EVM versus the input RF power is illustrated in seven cases: without the DPD, the DPD for up to third order nonlinearities, the DPD for up to third order nonlinearities with memory depth of one, the DPD for up to third order nonlinearities with memory depth of two, the DPD for up to fifth order nonlinearities, the DPD for up to fifth order nonlinearities with memory depth of one and the DPD for up to fifth order nonlinearities with memory depth of two. At the input RF power of -17.5 dBm, the DPD for up to third order nonlinearities results in an EVM improvement from -21.9 dB to -24.2 dB, i.e., 2.3 dB. When using the DPD for up to fifth order nonlinearities with memory depth of two, the EVM improvement becomes from -21.9 dB to -27.4 dB, i.e., 5.5 dB. It is seen that, further EVM improvements of up to 3.1 dB are achieved when the memory effect is considered for the input RF power of -15.5 dBm and -17.5 dBm. However, there is no improvement of EVM at other input

RF power. It can be seen that the memory effect in the WiFi over 10 km SMF transmission system is input RF power-sensitive.

Table 4-4 Extracted coefficients of the predistorter for WiFi over 10 SMF transmission system

Memory depth	$q = 0$	$q = 1$	$q = 2$
Up to third order nonlinearities	k_{10} = -0.8275	k_{11} = -0.4876	k_{12} = 0.1169
	k_{20} = 0.0951	k_{21} = -0.3503	k_{22} = -0.6065
	k_{30} = -0.2759	k_{31} = 0.1834	k_{32} = 0.5439
Up to Fifth order nonlinearities	k_{10} = -0.7259	k_{11} = -0.4337	k_{12} = 0.0935
	k_{20} = -1.0732	k_{21} = -1.1290	k_{22} = -0.5727
	k_{30} = 4.0291	k_{31} = 3.5393	k_{32} = 1.1305
	k_{40} = -6.3035	k_{41} = -5.5161	k_{42} = -1.7399
	k_{50} = 3.1733	k_{51} = 3.0368	k_{52} = 1.2562

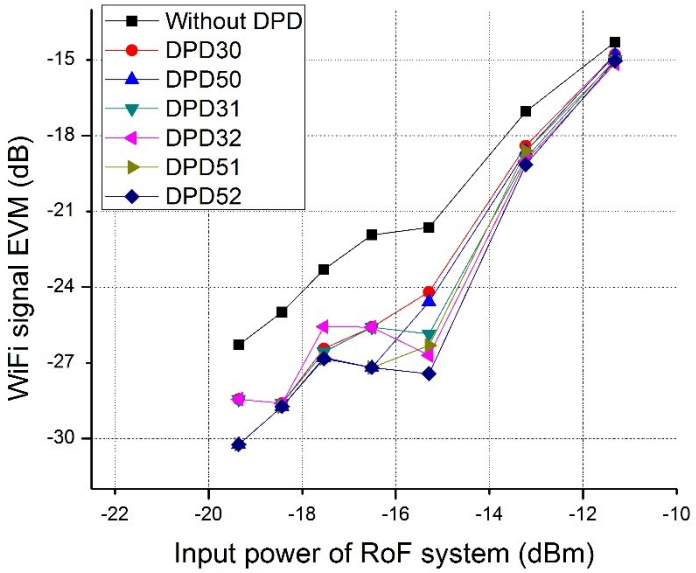

Figure 4-10 Measured EVM at the output of WiFi over 10 km SMF transmission system. DPD30: up to third order nonlinearities. DPD31: up to third order nonlinearities with one memory depth. DPD32: up to third order nonlinearities with two memory depths. DPD50: up to fifth order nonlinearities. DPD51: up to fifth order nonlinearities with one memory depth. DPD52: up to fifth order nonlinearities with two memory depths.

Figure 4-11 shows the comparison of signal constellation diagrams in the two cases: without the DPD and with the DPD for up to fifth order nonlinearities and memory depth of two, at the input RF power of -17.5 dBm, compared to (a) without the DPD, (b) with the DPD for up to fifth order nonlinearities with memory depth of two shows that the signal integrity is improved.

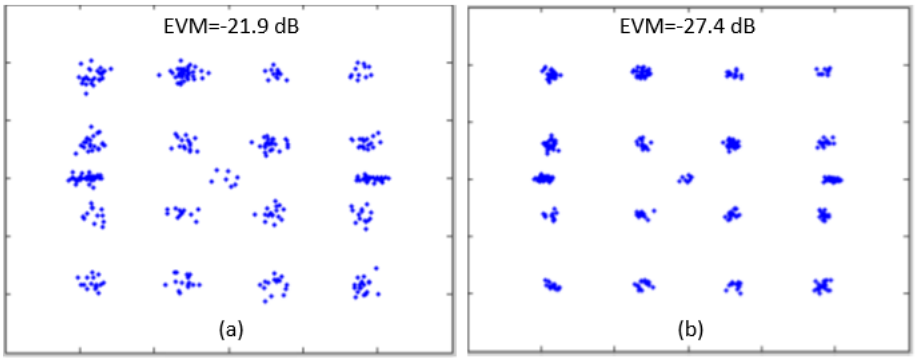

Figure 4-11 Measured constellation diagrams at the output of WiFi over 10 km SMF transmission system (a) without and (b) with the DPD for up to fifth order nonlinearities with two memory depths.

It is noticed that after adding 10 km SMF to the system, the improvements by using the DPD in WiFi over fiber transmission system are slightly reduced. The added SMF introduces optical nonlinear distortion to the RoF transmission system. Thus, compared to the output of BTB WiFi over fiber system, the output of WiFi over 10 km SMF transmission system includes nonlinear distortion introduced by the inlined optical, RF components and SMF. The improvements are slightly reduced by using the same DPD technique for WiFi over 10 km SMF transmission system.

4.3 DPD verifications in both WiFi & UWB over fiber systems

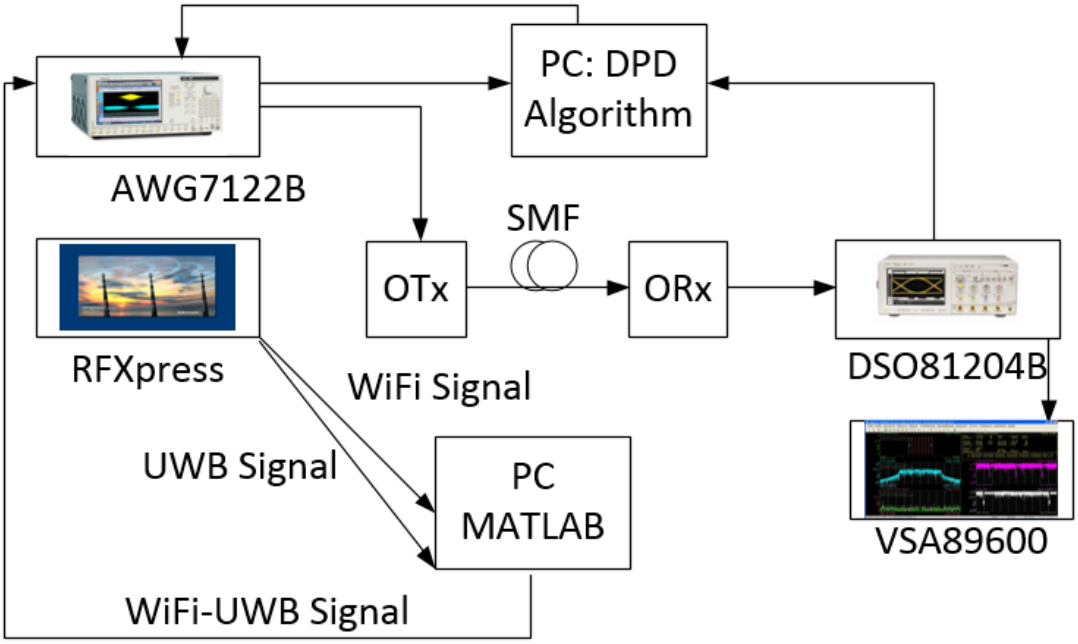

Figure 4-12 Experimental configuration of the DPD for both WiFi & UWB over fiber system

In Figure 4-12, a similar experimental configuration as mentioned in section 4.2 is used for the DPD verifications in both WiFi and UWB over fiber transmission system. Firstly, WiFi and UWB signal are created and extracted separately from RFXpress software and AWG7122B, and Matlab in a PC is used to combine the signals. Then the combined signal which occupies a bandwidth of over 2.4 GHz is sent to AWG7122B as the input of the RoF transmission system. The generated WiFi signal is the same as the one in previous experiment which follows IEEE 802.11a protocol. The generated UWB signal is centered at 3.96 GHz with data rate of 200 Mbit/s. It uses MB-OFDM which has 3 sub-bands. By using 128 subcarriers in each band, the subcarrier spacing is 4.125 MHz, UWB signal occupies the bandwidth of over 1.5 GHz. WiFi and UWB signals use 16 QAM and QPSK modulation schemes, respectively. After extracting the input and output RF signal data respectively from AWG7122B and DSO81204B, the Matlab offline signal processing in a

PC is carried out for extraction of the coefficients, and generation of the predistorted signal. Note that DPD is used for the whole transmission band. Still, two scenarios as mentioned in section 4.2 are included in optical signal transmission: BTB and 10 km SMF transmission between OTx and ORx. By comparing the EVM of received signal before and after applying the DPD for WiFi and UWB over fiber transmission systems, linearization performance is evaluated in VSA89600 of DSO81204B.

4.3.1 DPD verification in back to back WiFi and UWB over fiber system

Table 4-5 Extracted coefficients of the predistorter for BTB WiFi and UWB over fiber system

Up to third order nonlinearities	$k_{10} = 0.4772$
	$k_{20} = -0.1220$
	$k_{30} = 0.2793$
Up to fifth order nonlinearities	$k_{10} = 0.4709$
	$k_{20} = 0.3054$
	$k_{30} = -2.7631$
	$k_{40} = 6.8966$
	$k_{50} = -4.8834$

In the verification of the DPD for BTB WiFi and UWB over fiber transmission system, WiFi signal is firstly analyzed. Two cases are considered: up to third order nonlinearities and fifth order nonlinearities. The extracted coefficients of the predistorter for the above cases are given in Table 4-5. The DPD performance is shown in Figure 4-13, in which the measured EVM of WiFi signal versus the input RF power is given in three cases: without the DPD, the DPD for up to third order nonlinearities and the DPD for up to fifth order nonlinearities. After applying the DPD for BTB WiFi and UWB over fiber system, the measured EVM of WiFi signal is improved with the decrease of input RF power. However,

the improvement is reduced when system input power is low. So the performance of the DPD is still dependent on the system input RF power, and at the WiFi input power of -17.5 dBm, the DPD results in the best improvement, where the EVM of WiFi signal is improved from -23.9 dB to -28.4 dB, i.e., 4.5 dB improvement. It is seen that the increase of nonlinear order from third to fifth order does not lead to a significant improvement in linearization. It is because that the power of the fifth order nonlinearity is low.

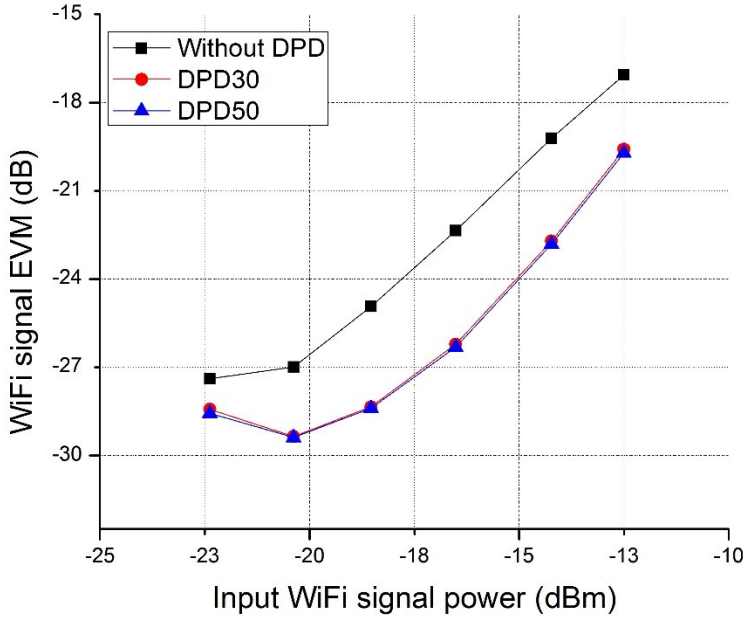

Figure 4-13 Measured EVMs of WiFi signal at the output of BTB WiFi and UWB over fiber system. DPD30: up to third order nonlinearities. DPD50: up to fifth order nonlinearities.

To give a clear impression on the improvement by the DPD, the signal constellations of the transmitted WiFi signal, i.e., 16QAM, at the system output are shown in Figure 4-14. By using the DPD for up to fifth order nonlinearities, the constellation diagram at the signal of -17.5 dBm is improved since the signal integrity are clearly better.

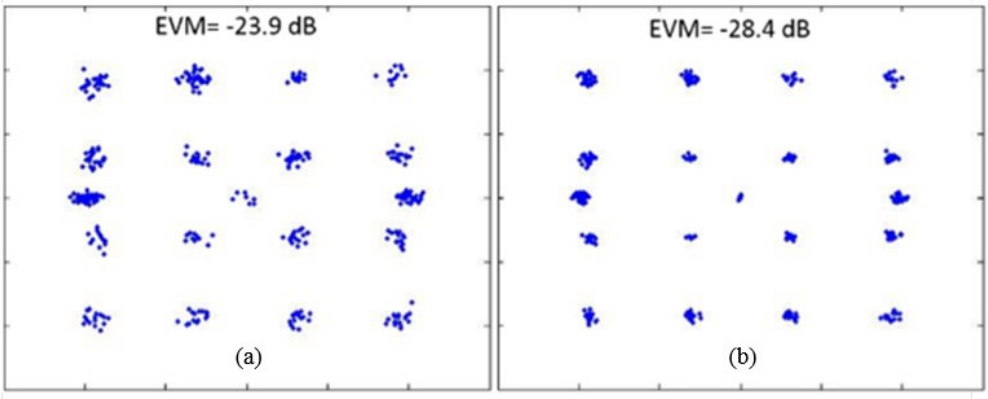

Figure 4-14 Measured constellation diagrams of WiFi signal at the output of BTB WiFi and UWB over fiber system (a) without and (b) with the DPD for up to fifth order nonlinearities.

Now we analyze the UWB signal, still, two cases are considered: up to third order and fifth order nonlinearities. By using the same extracted coefficients which are given in Table 4-5, the DPD performance is analyzed, as shown in Figure 4-15, in which the measured EVM of the UWB signal versus the input RF power is given in three cases: without the DPD, the DPD for up to third order nonlinearities and the DPD for up to fifth order nonlinearities. Again, the improvement by the DPD is dependent on the input RF power, and at the input RF power of -24.3 dBm, the DPD results in the best improvement, where the EVM of the UWB signal is improved from -24.3 dB to -28.9 dB, i.e., 4.6 dB improvement. It is seen that when the input RF power keeps decreasing, the improvement by the DPD is reduced. The possible reason could be: since the nonlinearity of the RoF transmission system is dependent on the input RF power, when the input RF power is reduced, the power of the nonlinearities of the system is low.

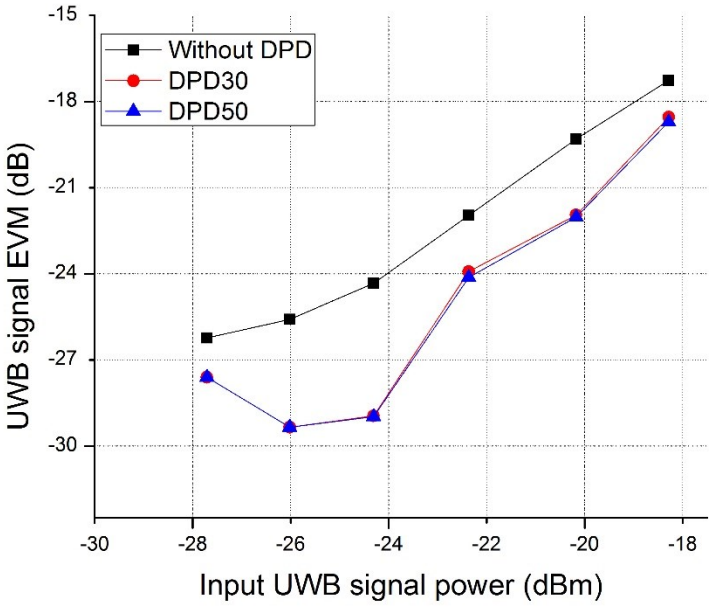

Figure 4-15 Measured EVMs of the UWB signal at the output of BTB WiFi and UWB over fiber system. DPD30: up to third order nonlinearities. DPD50: up to fifth order nonlinearities.

Figure 4-16 shows a comparison of the UWB signal constellation diagrams, i.e., QPSK. Two cases are presented: without the DPD and with the DPD for up to fifth order nonlinearities. At the input RF power of -24.3 dBm, the signal integrity is obviously improved since it is more concentrated.

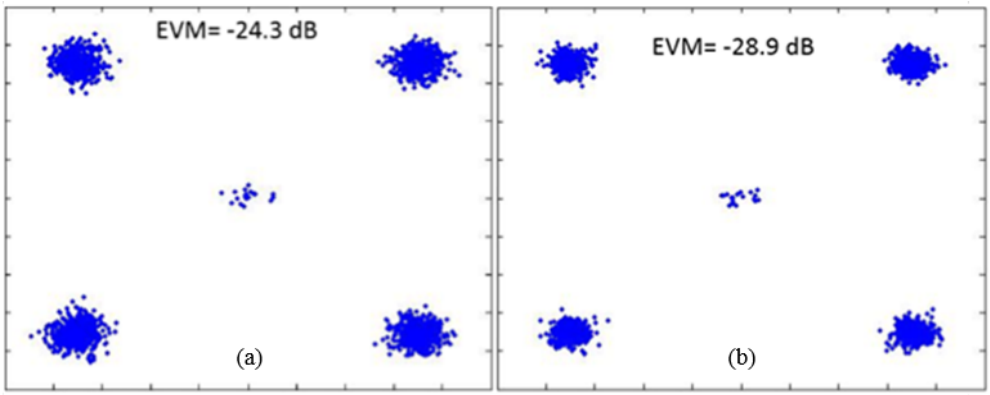

Figure 4-16 Measured constellation diagrams of the UWB signal at the output of BTB WiFi and UWB over fiber system (a) without and (b) with DPD for up to fifth order nonlinearities.

In this verification of the DPD for BTB WiFi and UWB over fiber transmission system, the EVM improvement of WiFi signal is not as good as in the previous experiment. Note that the WiFi and UWB signals are transmitted simultaneously in the RoF systems, more nonlinear components will be generated from the intermodulation between UWB subcarriers. Besides, intermodulation between WiFi subcarriers and UWB subcarriers will also introduce more nonlinear components. Thus, compared to the previous experiment, broadband RoF transmission system suffers from severer nonlinear distortions. By using the same DPD technique, improvements are reduced a little. However, according to the results, the DPD still provides decent improvements for the whole broad transmission band.

4.3.2 DPD verification for both WiFi and UWB over 10 km SMF transmission system

Table 4-6 Extracted coefficients of the predistorter for both WiFi and UWB over 10 km SMF transmisson system

Up to third order nonlinearities	$k_{10} = 0.2279$
	$k_{20} = -0.0860$
	$k_{30} = 0.1696$
Up to fifth order nonlinearities	$k_{10} = 0.2231$
	$k_{20} = 0.0117$
	$k_{30} = -0.3495$
	$k_{40} = 1.0017$
	$k_{50} = -0.6317$

For the verification of the DPD for both WiFi and UWB over 10 km SMF transmission system, two cases are considered: up to third order and fifth order nonlinearities. The extracted coefficients of the predistorter for the cases are given in Table 4-6. As shown in Figure 4-17, showing the measured EVM of WiFi signal versus the input RF power, the

performance of the DPD is shown in three cases: without the DPD, the DPD for up to third order nonlinearities and the DPD for up to fifth order nonlinearities. It is found that at input RF power of -18.6 dBm, the DPD provides the best improvement, where the EVM of WiFi signal is improved from -23.2 dB to -26.3 dB, i.e., 3.1 dB improvement. However, the improvement by the DPD for up to fifth order nonlinearities is not significant compared to the case of that for up to third order nonlinearities. The reason could be: compared to the third order nonlinearity, the power of the fifth order nonlinearity is much lower.

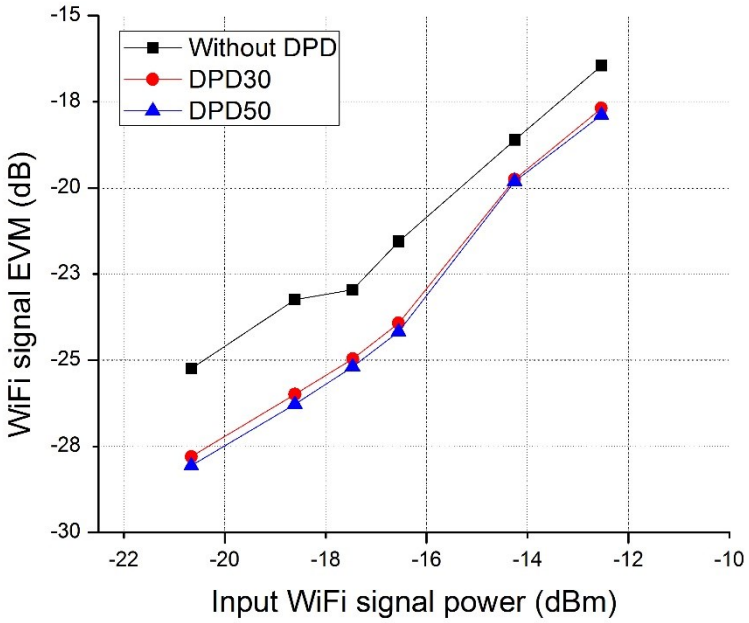

Figure 4-17 Measured EVMs of WiFi signal at output of both WiFi and UWB over 10 km SMF transmission system. DPD30: up to third order nonlinearities. DPD50: up to fifth order nonlinearities.

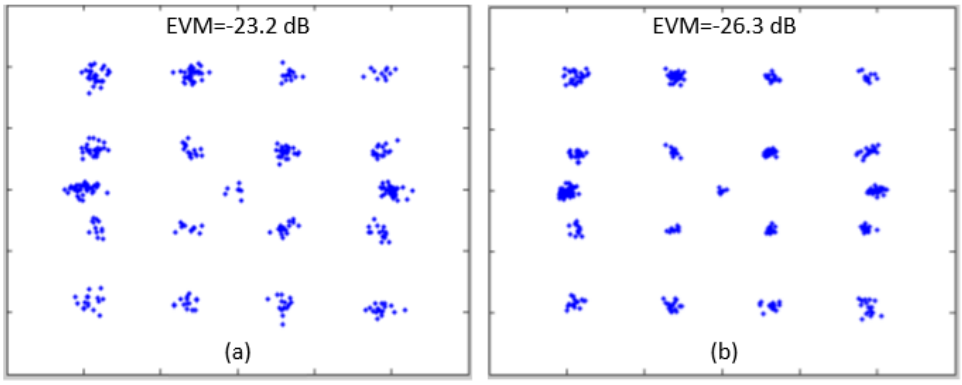

Figure 4-18 Measured constellation diagrams of WiFi signal at the output of WiFi & UWB over 10 km SMF transmission system (a) without and (b) with the DPD for up to fifth order nonlinearities.

To clearly show the improvement by the DPD, the signal constellation diagrams of the transmitted WiFi signal, i.e., 16QAM, at the system output are shown in Figure 4-18. By using the DPD for up to fifth order nonlinearities, the signal integrity at the input RF power of -18.6 dBm is improved.

Now we analyze the UWB signal, still, the same two cases are considered: up to third order and fifth order nonlinearities. By using the same extracted coefficients which are given in Table 4-6, the DPD performance is investigated, as shown in Figure 4-19, in which the measured EVM of the UWB signal versus the input RF power is given for the three cases: without the DPD, the DPD for up to third order nonlinearities and the DPD for up to fifth order nonlinearities. Again, the improvement by the DPD is dependent on the input RF power, and at the input RF power of -25.6 dBm, the DPD results in the best improvement, where the EVM of the UWB signal is improved from -21.9 dB to -25.9 dB, i.e., 4 dB improvement. It is seen that, the improvement by DPD is reduced when the input RF power is lower than -25.6 dBm, since the nonlinearity of the system is low.

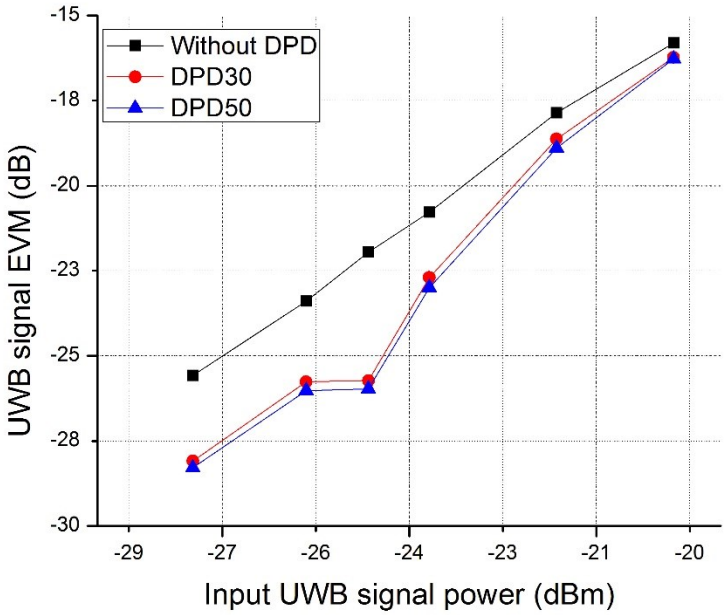

Figure 4-19 Measured EVMs of the UWB signal at the output of WiFi & UWB over 10 km SMF transmission system. DPD30: up to third order nonlinearities. DPD50: up to fifth order nonlinearities.

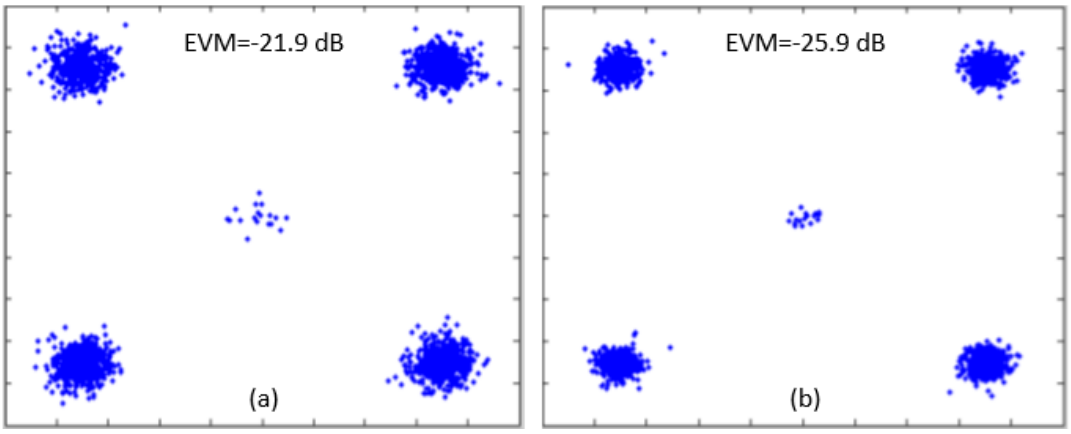

Figure 4-20 Measured constellation diagrams of the UWB signal at the output of both WiFi and UWB over 10 km SMF system (a) without and (b) with the DPD for up to fifth order nonlinearities.

Again, a comparison of the UWB signal constellation diagrams, i.e., QPSK, is shown in Figure 4-20. Two cases are presented: without the DPD and with the DPD for up to fifth order nonlinearities, at the input RF power of -25.6 dBm, the signal integrity is obviously improved since it is more concentrated.

Memory effect also has been included in the DPD verification in the WiFi and UWB over fiber systems. However, almost no improvement was achieved. For example, the improvements of the EVM were almost the same in the cases: the DPD for up to fifth order nonlinearities and the DPD for up to fifth order nonlinearities with memory depth of two. Thus, no detailed memory effect included verification is given in this section. Compared to the output of WiFi over fiber transmission system, extra nonlinearities included in the output of WiFi and UWB over 10 km SMF transmission system are: optical nonlinearities introduced by SMF, nonlinear distortion introduced by the intermodulation between the UWB subcarriers and nonlinear distortion introduced by the intermodulation between the WiFi and UWB subcarriers. Thus, more RF nonlinear distortions and severer optical nonlinearities in SMF are induced in WiFi and UWB over fiber transmission systems, the memory effect of WiFi over fiber transmission systems is relatively lower, the improvements are reduced by using DPD for WiFi and UWB over 10 km SMF transmission system.

Chapter 5 Conclusion

5.1 Thesis conclusion

RoF supports the broad bandwidth and transparent infrastructure that is able to support diverse wireless technologies. However, the directly modulated RoF transmission system which is based on optical subcarrier modulation, is vulnerable to nonlinear distortions. Compared to optical linearization and analog predistortion methods, DPD provides a more adaptive and precise solution in linearization of RoF transmission systems. In this thesis, the DPD technique implemented in RF domain is investigated for broadband RoF transmission systems. Both nonlinear distortions and memory effects are included in memory polynomial model, which is used to model the nonlinear RoF systems. After using least square (LS) method to extract the coefficients of the predistorter, the trained predistorter is implemented and then verified in two experiments of directly modulated RoF transmission systems.

In the first experiment, the DPD is verified in WiFi over fiber transmission systems. The EVM improvements of 8.2 dB and 5.6 dB are achieved in BTB and after 10 km single mode fiber (SMF) transmission, respectively. When memory effect is included, compared to the situation without memory effect, further 3 dB and 3.1 dB EVM improvements are achieved in BTB and after 10 km SMF transmission.

In the second experiment, the DPD is verified in both WiFi and ultra wide band (UWB) over fiber transmission systems. WiFi and UWB signals are centered at 2.4 and 3.96 GHz, respectively, and the combined transmission bandwidth is over 2.4 GHz. It is shown that the implemented DPD leads to EVM improvements of 4.5 dB (BTB) and 3.1 dB (10 km

SMF) for the WiFi signal, and 4.6 dB (BTB) and 4 dB (10 km SMF) for the UWB signal simultaneously.

Note that EVM improvements using the implemented DPD are slightly reduced when 10 km SMF is added to the RoF transmission systems. This is because the added SMF introduce optical nonlinear distortions to RoF transmission systems. Also, note that when the same DPD is implemented at a larger bandwidth, EVM improvements are reduced a little. When both WiFi and UWB signals are transmitted in the broadband RoF system simultaneously, the intermodulation between UWB subcarriers and the intermodulation between WiFi subcarriers and UWB subcarriers introduces more nonlinear distortions. The improvements are reduced in DPD for WiFi and UWB over fiber transmission systems.

Furthermore, the RF domain based DPD linearization technique has the advantage of better computational efficiency.

5.2 Future work

Future research on DPD techniques over broadband RoF transmission system will be:

Firstly, in this work, the performance of DPD for WiFi over fiber transmission systems improves, when considering memory effect at some of the input power. However, in WiFi and UWB over fiber transmission system, by considering memory effect at some of the input power. However, in the verification of DPD for both WiFi and UWB over fiber systems, when the memory effects are included, almost no further improvements from the implemented DPD is found. Digital filter assisted digital linearization may be better to attack memory effect. So further research on this topic needs to be investigated in order to have better results at large bandwidths.

Secondly, since the improvements of DPD for simultaneously transmitted signals are realized, the implemented DPD is able to linearize the broadband RoF transmission systems. Still, linearization for an RoF link to transmit more RF signals in a larger bandwidth needs to be verified.

Thirdly, compared to the previous DPD techniques, by considering the same nonlinear order and memory effect, only half of the number of coefficients are calculated in the implemented DPD technique. However, the improvements of the implemented DPD are reduced when 10 km SMF is added to the RoF transmission systems. To achieve better improvements, the modeling of optical nonlinear distortions introduced by SMF in DPD techniques needs to be investigated in the future work.

Reference

[1] Xiupu Zhang, Ran Zhu, Dongyan Shen, Taijun Liu, 'Linearization technologies for broadband Radio-over-Fiber transmission systems', *Photonics,* vol.1, no. 4, pp. 455-472, Nov. 2014.

[2] A.J.Cooper, 'Fibre/radio for the provision of cordless mobile telephony services in the access network', *Electronics letters*, vol. 26 no. 24, pp. 2054 – 2056, Nov. 1990.

[3] Arun Joseph, Shanthi Prince, 'Performance analysis and optimization of radio over fiber link', *International Conference on Communications and Signal Processing (ICCSP)*, pp. 1599 – 1604, Apr. 2014.

[4] U. Sampath Kumar, V. Saminadan and P. Williams, 'Performance evaluation of millimeter wave and UWB signals over fiber radio networks', *International Conference on Communications and Signal Processing (ICCSP)*, pp. 104 – 107, Apr. 2012.

[5] Ehsan Dadrasnia, Faisal Rafiq Mahamd Adikan, 'DWDM effects of single model optical fiber in radio over fiber system', *International Conference on Electronic Computer Technology (ICECT)*, pp.39-41, May 2010.

[6] George S. D. Gordon, Michael J. Crisp, Richard V. Penty, Timothy D. Wilkinson, Ian H. White, 'Feasibility demonstration of a mode-division multiplexed MIMO-enabled Radio-over-Fiber distributed antenna system', *Journal of Lightwave Technology*, vol. 32, no. 20, pp. 3521 – 3528, Mar. 2014.

[7] Y.Yang, F. li, C. Lim, A. Nirmalathas, 'Radio-over-fiber technologies for future mobile backhaul supporting cooperative base stations', *IEEE MTT-S International Microwave Symposium Digest (IMS)*, pp 1 – 3, Jun. 2013.

[8] David Wake, Keith Beacham, 'A novel switched radio over fiber architecture for distributed antenna systems', *The 17th Annual Meeting of the IEEE Lasers and Electro-Optics Society,* vol.1, pp 55-56, Nov. 2014.

[9] J. Park, W.V. Sorin and K.Y. Lau, 'Elimination of the fibre chromatic dispersion penalty on 1550 nm millimetre-wave optical transmission', *Electronics Letters*, vol. 33, no. 6, pp 512-513, Mar. 1997.

[10] G.H. Smith, D. Novak and Z. Ahmed, 'Technique for optical SSB generation to overcome dispersion penalties in fibre-radio systems', *Electronics Letters,* vol. 33, no. 1, pp. 74-75, Jan. 1997.

[11] Ron Chase, 'UWB: fostering innovation through a balanced regulatory framework', *Federal Communication Commission (FCC)*, pp.13, Apr. 2006.

[12] Matthew L. Welborn, 'System considerations for ultra-wideband wireless networks', *IEEE Radio and Wireless Conference*, pp. 5-8, Aug. 2001.

[13] David M. Pozar , *Microwave Engineering*, 3rd ed., 2005, John Wiley & sons, Inc.

[14] Bouchaib Hraimel, Xiupu Zhang, Wei Jiang, Ke Wu, Taijun Liu, Tiefeng Xu, Qiuhua Nie, Kun Xu, 'Experimental demonstration of mixed-polarization to linearize electro-absorption modulators in Radio-over-Fiber links', *IEEE Photonics Technology Letters*, vol. 23, no. 4, pp 230 – 232, Dec. 2010.

[15] Biagio Masella, Bouchaib Hraimel, Xiupu Zhang, 'Enhanced spurious-free dynamic range using mixed polarization in optical single sideband Mach–Zehnder modulator', *Journal of Lightwave Technology,* vol. 27, no. 15, pp. 3034 – 3041, Aug. 2009.

[16] Ran Zhu, Xiupu Zhang 'Linearization of radio-over-fiber systems by using two lasers with different wavelengths', *International Microwave Symposium (IMS), IEEE MTT-S,* pp. 1-3, Jun. 2014.

[17] Gordon C. Wilson, Thomas H. Wood, M. Gans, J. L. Zyskind, J. W. Sulhoff, J. E. Johnson,T. Tanbun-Ek, Paul A. Mortan 'Predistortion of electro-absorption modulators for analog CATV systems at 1.55 μm', *Journal of Lightwave Technology,* vol. 15, no. 9, pp. 1654 – 1662, Aug. 2002.

[18] Yiming Shen, Bouchaib Hraimel, Xiupu Zhang, Glenn E. R. Cowan, Ke Wu, Taijun Liu, 'A novel analog broadband RF predistortion circuit to linearize electro-absorption modulators in multiband OFDM Radio-over-Fiber systems', *IEEE Transactions on Microwave Theory and Techniques*, vol. 58, no. 11, pp. 3327 – 3335, Nov. 2010.

[19] Ran Zhu, Zichen Xuan, Ye Zhang, Xiupu Zhang and Dongya Shen, 'Novel broadband analog predistortion circuit for radio-over-fiber systems', *IEEE MTT-S International Microwave Symposium (IMS), 2015*, pp. 1-4, May 2015.

[20] Luis C. Vieira, Nathan J. Gomes, Anthony Nkansah, Frédéric van Dijk, 'Behavioral modeling of radio-over-fiber links using memory polynomials', *IEEE Topical Meeting on Microwave Photonics (MWP)*, pp. 85-88, Oct. 2010.

[21] Hao Chen, Jianqiang Li, Kun Xu, Yinqing Pei, Yitang Dai, Feifei Yin, and Jintong Lin, 'Experimental investigation on multi-dimensional digital predistortion for linearization in multi-band radio-over-fiber systems', *Optical Fiber Communications Conference and Exhibition (OFC)*, pp. 1-3, Mar. 2014.

[22] Oluyemi Omomukuyo, Manoj P. Thakur and John E. Mitchell, 'Experimental demonstration of digital predistortion for linearization of Mach-Zehnder modulators in

direct detection MB-OFDM ultra-wideband over fiber systems', *Communications and Photonics Conference (ACP)*, pp.1-3, Nov. 2012.

[23] Yinqing Pei, Kun Xu, Jianqiang Li, Anxu Zhang, Yitang Dai, Yuefeng Ji, Jintong Lin, 'Complexity-reduced digital predistortion for subcarrier multiplexed radio over fiber systems transmitting sparse multi-band RF signals', *Optical Express*, vol. 21, no. 3, pp. 3708-14, Feb. 2013.

[24] Gang Cao, Tiefeng Xu, Taijun Liu, Yan Ye, Hao Lin, Xiaojun Luo, Liang Li, 'Memory polynomial based adaptive predistortion for Radio-over-Fiber systems', *International Conference on Microwave and Millimeter Wave Technology (ICMMT)*, vol. 2, pp. 1-4, May 2012.

[25] Atso Hekkala, Mikko Hiivala, Mika Lasanen, Jari Perttu, Luis C. Vieira, Nathan J. Gomes, Anthony Nkansah, 'Predistortion of Radio-over-Fiber links: algorithms, implementation, and measurements', *IEEE Transactions on Circuits and Systems I: Regular Papers*, vol. 59, no. 3, pp. 664 – 672, Feb. 2012.

[26] Zhansheng Liu, Manuel Alberto Violas, and Nuno Borges Carvalho, 'Transmission of four channels SCM over fiber and nonlinear compensation for RSOA external modulators', *IEEE GLOBECOM Workshops*, pp. 147-151, Dec. 2011.

[27] Chin Hee Lee, Vas Postoyalko, Tim O'Farrell, 'Enhanced performance of RoF link for cellular mobile systems using postdistortion compensation', *15th IEEE International Symposium on Personal, Indoor and Mobile Radio Communications*, vol.4, pp. 2772 – 2776, Sept. 2004.

[28] Yinqing Pei, Jianqiang Li, Kun Xu, Yitang Dai, Yuefeng Ji and Jintong Lin, 'Digital multi-channel post-linearization for uplink in multi-band radio-over-fiber

systems', *Optical Fiber Communications Conference and Exhibition (OFC), 2014*, pp. 1-3, Mar. 2014.

[29] Xavier N. Fernando, Abu B. Sesay, 'Adaptive asymmetric linearization of Radio-over-Fiber links for wireless access', *IEEE Transactions on Vehicular Technology*, vol.51, no. 6, pp. 1576 – 1586, Feb. 2003.

[30] Yan Cui, Yitang Dai, Feifei Yin, Qiang Lv, Jianqiang Li, Kun Xu, Jintong Lin, 'Enhanced spurious-free dynamic range in intensity-modulated analog photonic Link using digital post processing', *IEEE Photonics Journal*, vol.6, no.2, Mar. 2014.

[31] Lei Ding, Tong Zhou, Dennis R. Morgan, Zhengxiang Ma, J. Stevenson Kenney, Jaehyeong Kim and Charles R. Giardina, 'A robust digital baseband predistorter constructed using memory polynomials', *IEEE Transactions on Communications*, vol.52, no.1, pp. 159 – 165, Mar. 2004.

[32] Ying Liu, Wensheng Pan, Shihai Shao, Youxi Tang, 'A general digital predistortion architecture using constrained feedback bandwidth for wideband power amplifiers', *IEEE Transactions on Microwave Theory and Techniques*, vol.63, no.5, pp. 1544 – 1555, Mar. 2015.

[33] Nikolai Wolff, Olof Bengtsson, and Wolfgang Heinrich, 'Complexity of DPD linearization in the full RF-band for a WiMAX power amplifier', 2015 German Microwave Conference (GeMiC), pp.13-16, Mar. 2015.

[34] Oualid Hammi, Andrew Kwan, Souheil Bensmida, Kevin A. Morris, Fadhel M. Ghannouchi, 'A digital predistortion system with extended correction bandwidth with application to LTE-A nonlinear power amplifiers', *IEEE Transactions on Circuits and Systems I: Regular Papers*, vol.61, no.12, pp. 3487 – 3495, Sept. 2014.

[35] Georges Karam, Hikmat Sari, 'Data predistortion techniques using inter symbol interpolation', *IEEE Transactions on Communications*, vol. 38, no. 10, pp. 1716-1723, Oct. 1990.

[36] A. A. M. Saleh and J. Salz, 'Adaptive linearization of power amplifiers in digital radio systems', *The Bell System Technical Journal*, vol.62, no.4, pp.1019-1033, Apr. 1983.

[37] Christopher J. Clark, George Chrisikos, Michael S. Muha, Andrew A. Moulthrop, Christopher P. Silva, 'Time-domain envelope measurement technique with application to wideband power amplifier modeling', *IEEE Transactions on Microwave Theory and Techniques*, vol.46, no.12, pp. 2531-2540. Dec. 1998.

[38] Hyun Woo Kang, Yong Soo Cho, Dae Hee Youn, 'On compensating nonlinear distortions of an OFDM system using an efficient adaptive predistorter', *IEEE transactions on communications*, vol. 47, no. 4, pp. 522-526, Apr. 1999.

[39] S. Benedetto, E. Biglieri, 'Nonlinear equalization of digital satellite channels', *IEEE Journal on Selected Areas in Communications*, vol. 1, no. 1, pp. 57-62, Jan. 1983.

[40] Bilel Fehri, Slim Boumaiza, 'Baseband equivalent volterra series for behavioral modeling and digital predistortion of power amplifiers driven with wideband carrier aggregated signals', *IEEE Transactions on Microwave Theory and Techniques*, vol. 62, no. 11, pp. 2594 – 2603, Nov. 2014.

[41] J. Kim, K. Konstdntinou, 'Digital predistortion of wideband signals based on power amplifier model with memory', *Electronics Letters*, vol. 37, no. 23, pp. 1417 – 1418, Aug. 2002.

[42] MITEQ, ‘GHz amplifiers go nano’, *Electronics Letters*, vol. 47, no. 4, pp. 227, Feb. 2011.